J. Fluid Mech. (2016), *vol.* 786, *pp.* 154–189.
doi:10.1017/jfm.2015.587

Linear and nonlinear receptivity of the boundary layer in transonic flows

A. I. Ruban[1,†], T. Bernots[1] and M. A. Kravtsova[1]

[1]Department of Mathematics, Imperial College London, 180 Queen's Gate, London SW7 2BZ, UK

(Received 1 April 2015; revised 25 August 2015; accepted 4 October 2015;
first published online 30 November 2015)

In this paper we analyse the process of the generation of Tollmien–Schlichting waves in a laminar boundary layer on an aircraft wing in the transonic flow regime. We assume that the boundary layer is exposed to a weak acoustic noise. As it penetrates the boundary layer, the Stokes layer forms on the wing surface. We further assume that the boundary layer encounters a local roughness on the wing surface in the form of a gap, step or hump. The interaction of the unsteady perturbations in the Stokes layer with steady perturbations produced by the wall roughness is shown to lead to the formation of the Tollmien–Schlichting wave behind the roughness. The ability of the flow in the boundary layer to convert 'external perturbations' into instability modes is termed the receptivity of the boundary layer. In this paper we first develop the linear receptivity theory. Assuming the Reynolds number to be large, we use the transonic version of the viscous–inviscid interaction theory that is known to describe the stability of the boundary layer on the lower branch of the neutral curve. The linear receptivity theory holds when the acoustic noise level is weak, and the roughness height is small. In this case we were able to deduce an analytic formula for the amplitude of the generated Tollmien–Schlichting wave. In the second part of the paper we lift the restriction on the roughness height, which allows us to study the flows with local separation regions. A new 'direct' numerical method has been developed for this purpose. We performed the calculations for different values of the Kármán–Guderley parameter, and found that the flow separation leads to a significant enhancement of the receptivity process.

Key words: boundary layer receptivity, boundary layer separation, high-speed flow

1. Introduction

The phenomenon of laminar–turbulent transition has been under the close attention of researchers for more than a century, and still remains one of the central problems of fluid dynamics. In addition to its importance from a fundamental viewpoint, a resolution of this problem is also necessary for practical applications. In particular, when dealing with aerodynamic applications, one has to predict the 'position' of the laminar–turbulent transition on the aircraft wing, which is impossible without an accurate description of the receptivity process.

† Email address for correspondence: a.ruban@imperial.ac.uk

The laminar–turbulent transition is a very complicated phenomenon, and it is known to proceed differently in different flows. In aerodynamic flows it follows a classical scenario with a succession of well-defined stages. In the first stage the external perturbation (such as free-stream turbulence, acoustic noise, wall roughnesses, wall vibrations, etc.) penetrate the boundary layer and turn into the boundary-layer instability modes: Tollmien–Schlichting waves, cross-flow vortices or Taylor–Görtler vortices. In real flight conditions, the external perturbations are very weak – in fact, significantly weaker compared even to specially designed 'low-turbulence' wind tunnels. Therefore, the initial amplitude of instability modes generated in the boundary layer is small, and cannot cause laminar–turbulent transition. Before this happens, the perturbations have to amplify further downstream. This is considered to be the second stage of the transition process. When the amplitude of the perturbations reaches a certain level, nonlinear effects come into play (third stage), and then a rapid transition to a turbulent state is observed. This means that the e^N method, currently adopted by the aerospace industry, is insufficient for accurate prediction of the transition. It does not account for environmental noise and wing surface roughness, which are well known to significantly influence the position of the transition. The receptivity theory aims to establish a link between the external perturbations and the laminar–turbulent transition, and serves the following purposes: (i) to identify the perturbations that can easily penetrate the boundary layer and turn into instability modes, (ii) to calculate the initial amplitude of the instability modes, and (iii) to devise the means to control the transition process through suppression of the boundary-layer receptivity. The second of these tasks can be performed using various mathematical tools, including the numerical solution of the linearised Navier–Stokes equations. However, it is the asymptotic approach that proves to be instrumental in performing tasks (i) and (iii).

The first paper, where the triple-deck theory was used to study the receptivity of the boundary layer, was published by Terent'ev (1981). This study considered an incompressible fluid flow past a flat plate with the basic steady flow given by the Blasius solution. It was assumed that a short section of the plate surface performed periodic vibrations in the direction perpendicular to the wall. In order to ensure that the flow is described by the triple-deck theory, the frequency of the vibrations was chosen to be $\omega = O(Re^{1/4})$ and the length of the vibrating section $\Delta x = O(Re^{-3/8})$. Terent'ev's formulation represents a simplified mathematical model of the classical experiments by Schubauer & Skramstad (1948), where the Tollmien–Schlichting waves were generated by a vibrating ribbon. Terent'ev was able to determine the amplitude of the generated Tollmien–Schlichting waves as a function of the amplitude and shape of the vibrating part of the wall.

The effect of acoustic noise on the boundary layer was first considered by Goldstein (1983), who studied the Blasius boundary-layer flow on a flat plate and used the fact that this flow is non-parallel near the leading edge of the plate. He showed that, when an acoustic wave interacts with the leading-edge region, the Lam–Rott eigensolutions are generated. Goldstein (1983) noticed, however, that these eigensolutions decay exponentially before becoming Tollmien–Schlichting waves further downstream.

For effective generation of Tollmien–Schlichting waves, the external perturbations have to satisfy rather restrictive resonance conditions. Unlike in a simple mechanical system, say, a pendulum, where the resonance is observed provided that the frequency of the external forcing is close to the natural frequency of the pendulum oscillations, in fluid flows resonance implies that, in addition to the frequency, the wavenumber of the external perturbations should also be close to that of the Tollmien–Schlichting waves. Ruban (1984) and Goldstein (1985) were the first to demonstrate how this

double-resonance principle can be used in the receptivity theory. It is known from Lin (1946) and Smith (1979*a*,*b*) that, in the boundary layer in a subsonic flow, the frequency of the Tollmien–Schlichting waves on the lower branch of the neutral curve is an $O(Re^{1/4})$ quantity, and the wavelength is $O(Re^{-3/8})$. This means that in the 'vibrating ribbon' problem considered by Terent'ev (1981) the two resonance conditions are satisfied automatically. The situation is more complex in the case of the boundary-layer receptivity to acoustic noise, which was analysed by Ruban (1984) and Goldstein (1985). They were interested in the generation of the Tollmien–Schlichting waves in the boundary layer at a finite distance from the leading edge, where the Tollmien–Schlichting waves become unstable. To satisfy the first resonance condition, the frequency of the acoustic wave was chosen to be an $O(Re^{1/4})$ quantity, but then the wavelength of the acoustic wave appears to be $O(Re^{-1/4})$ long, which is much longer than the wavelength of the Tollmien–Schlichting wave. Hence, the acoustic wave alone is insufficient for Tollmien–Schlichting wave generation. To satisfy the resonance condition with respect to the wavenumber, the acoustic wave has to come into interaction with wall roughnesses, which are, of course, plentiful on a real aircraft wing. Ruban (1984) and Goldstein (1985) demonstrated that the interaction of an acoustic wave with such roughnesses produces Tollmien–Schlichting waves in the boundary layer. An explicit formula for the amplitude of the generated Tollmien–Schlichting waves was deduced.

A review of subsequent studies in this field can be found in a recent paper of Ruban, Bernots & Pryce (2013) that is devoted to the analysis of the generation of Tollmien–Schlichting waves by vibrations of the wing surface.

Here, in the present paper, our attention is with the receptivity of the boundary layer to acoustic noise in transonic flows; the latter represent the cruise flight conditions of modern passenger aircraft. In our study we rely on the asymptotic description of the Tollmien–Schlichting waves in transonic flow, given by Timoshin (1990), by Bowles & Smith (1993) and more recently by Bogdanov *et al.* (2010). In addition to developing the linear receptivity theory, we also study the influence of nonlinear effects on the generation of the Tollmien–Schlichting waves.

2. Problem formulation

Let us consider the flow of a perfect gas past a flat plate. We shall assume for simplicity that the plate is parallel to the free-stream velocity, and upstream of the plate the flow is uniform (see figure 1). We shall further assume that there is a plane acoustic wave travelling parallel to the plate. The flow analysis will be conducted using the compressible Navier–Stokes equations, which are presented here retaining only the main viscous terms in the momentum and energy equations:

$$\hat{\rho}\left(\frac{\partial\hat{u}}{\partial\hat{t}}+\hat{u}\frac{\partial\hat{u}}{\partial\hat{x}}+\hat{v}\frac{\partial\hat{u}}{\partial\hat{y}}\right)=-\frac{\partial\hat{p}}{\partial\hat{x}}+\frac{\partial}{\partial\hat{y}}\left(\hat{\mu}\frac{\partial\hat{u}}{\partial\hat{y}}\right)+\cdots, \tag{2.1a}$$

$$\hat{\rho}\left(\frac{\partial\hat{v}}{\partial\hat{t}}+\hat{u}\frac{\partial\hat{v}}{\partial\hat{x}}+\hat{v}\frac{\partial\hat{v}}{\partial\hat{y}}\right)=-\frac{\partial\hat{p}}{\partial\hat{y}}+\frac{\partial}{\partial\hat{y}}\left(\hat{\mu}\frac{\partial\hat{v}}{\partial\hat{y}}\right)+\cdots, \tag{2.1b}$$

$$\hat{\rho}\left(\frac{\partial\hat{h}}{\partial\hat{t}}+\hat{u}\frac{\partial\hat{h}}{\partial\hat{x}}+\hat{v}\frac{\partial\hat{h}}{\partial\hat{y}}\right)=\frac{\partial\hat{p}}{\partial\hat{t}}+\hat{u}\frac{\partial\hat{p}}{\partial\hat{x}}+\hat{v}\frac{\partial\hat{p}}{\partial\hat{y}}+\frac{1}{Pr}\frac{\partial}{\partial\hat{y}}\left(\hat{\mu}\frac{\partial\hat{h}}{\partial\hat{y}}\right)+\hat{\mu}\left(\frac{\partial\hat{u}}{\partial\hat{y}}\right)^2+\cdots, \tag{2.1c}$$

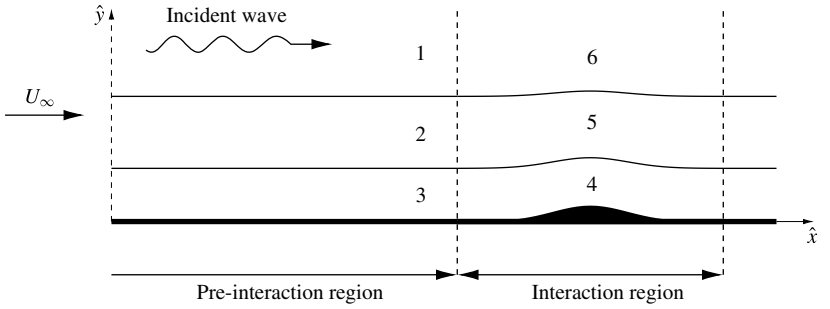

FIGURE 1. Illustration of the flow structure for the acoustic wave receptivity.

$$\frac{\partial \hat{\rho}}{\partial \hat{t}} + \frac{\partial(\hat{\rho}\hat{u})}{\partial \hat{x}} + \frac{\partial(\hat{\rho}\hat{v})}{\partial \hat{y}} = 0, \tag{2.1d}$$

$$\hat{h} = \frac{\gamma}{\gamma - 1}\frac{\hat{p}}{\hat{\rho}}. \tag{2.1e}$$

We shall use Cartesian coordinates with $\hat{x}$ measured along the plate surface from the leading edge, and $\hat{y}$ in the perpendicular direction. The dimensional velocity components are denoted as $(\hat{u}, \hat{v})$ and $\hat{t}$ is the time. We further denote the gas density by $\hat{\rho}$, the pressure by $\hat{p}$, the enthalpy by $\hat{h}$ and the dynamic viscosity coefficient by $\hat{\mu}$; Pr is the Prandtl number and γ is the ratio of specific heats.

Let U_∞ be the free-stream velocity and L the distance from the leading edge to the roughness. The values of the pressure, density and viscosity coefficient in the free stream are denoted by p_∞, ρ_∞ and μ_∞, respectively. The Reynolds number is defined as

$$Re = \frac{\rho_\infty U_\infty L}{\mu_\infty}, \tag{2.2}$$

and is assumed to be large.

To perform the asymptotic analysis of the Navier–Stokes equations at large values of Re, one needs to identify the resonance frequency ω of the acoustic wave and the characteristic length ℓ of the wall roughness. As has already been mentioned, in subsonic flow

$$\omega = O(Re^{1/4}), \quad \ell = O(Re^{-3/8}). \tag{2.3a,b}$$

To deduce the corresponding estimates for the transonic flow, one can proceed as follows. It is known that, in subsonic flow, the frequency and the wavelength of the neural Tollmien–Schlichting wave depend on the Mach number M_∞ as follows:

$$\omega \sim Re^{1/4}(1 - M_\infty^2)^{1/4}, \quad \ell \sim Re^{-3/8}(1 - M_\infty^2)^{-3/8}. \tag{2.4a,b}$$

Keeping this in mind, Timoshin (1990) assumed that $M_\infty - 1$ becomes progressively smaller and analysed the equations in the three tiers of the triple-deck model. He found that the triple-deck equations remain unchanged for all $1 - M_\infty^2 \gg Re^{-1/9}$. However, when $1 - M_\infty^2$ becomes a quantity of order $O(Re^{-1/9})$, the flow in the upper deck can no longer be described by the Laplace equation. It has to be replaced by the transonic small-perturbation equation.

Consequently, we shall assume that the free-stream Mach number M_∞ is such that (see Timoshin 1990; Bowles & Smith 1993)

$$M_\infty^2 = 1 + Re^{-1/9} Q_\infty, \tag{2.5}$$

where Q_∞ is assumed to be an order-one quantity. It is referred to as the Kármán–Guderley parameter. Substitution of (2.5) into (2.4) shows that in the transonic flow the resonance conditions are achieved when

$$\omega \sim Re^{2/9}, \quad \ell \sim Re^{-1/3}. \tag{2.6a,b}$$

3. Flow ahead of the wall roughness

Here we shall consider the steady boundary layer that forms on the plate surface, and the perturbations produced in this flow by a weak acoustic wave travelling along the plate.

3.1. *Steady compressible boundary-layer flow*

The solution of the Navier–Stokes equations (2.1) for the steady flow in the boundary layer is represented in the form of the following asymptotic expansions:

$$\hat{u} = U_\infty U_0(\breve{x}, \bar{Y}) + \cdots, \quad \hat{\rho} = \rho_\infty R_0(\breve{x}, \bar{Y}) + \cdots, \tag{3.1a,b}$$

$$\hat{v} = U_\infty Re^{-1/2} V_0(\breve{x}, \bar{Y}) + \cdots, \quad \hat{h} = U_\infty^2 H_0(\breve{x}, \bar{Y}) + \cdots, \tag{3.1c,d}$$

$$\hat{p} = p_\infty + \rho_\infty U_\infty^2 Re^{-1/2} p'(\breve{x}, \bar{Y}) + \cdots, \quad \hat{\mu} = \mu_\infty \mu_0(\breve{x}, \bar{Y}) + \cdots. \tag{3.1e,f}$$

Here the dimensionless coordinates $(\breve{x}, \bar{Y})$ are introduced through the scalings

$$\hat{x} = L\breve{x}, \quad \hat{y} = LRe^{-(1/2)}\bar{Y}. \tag{3.2a,b}$$

Substitution of (3.1) and (3.2) into the Navier–Stokes equations (2.1) leads to the classical boundary-layer equations for compressible flow:

$$R_0 U_0 \frac{\partial U_0}{\partial \breve{x}} + R_0 V_0 \frac{\partial U_0}{\partial \bar{Y}} = \frac{\partial}{\partial \bar{Y}} \left(\mu_0 \frac{\partial U_0}{\partial \bar{Y}} \right), \tag{3.3a}$$

$$R_0 U_0 \frac{\partial H_0}{\partial \breve{x}} + R_0 V_0 \frac{\partial H_0}{\partial \bar{Y}} = \frac{1}{Pr} \frac{\partial}{\partial \bar{Y}} \left(\mu_0 \frac{\partial H_0}{\partial \bar{Y}} \right) + \mu_0 \left(\frac{\partial U_0}{\partial \bar{Y}} \right)^2, \tag{3.3b}$$

$$U_0 \frac{\partial R_0}{\partial \breve{x}} + R_0 \frac{\partial V_0}{\partial \bar{Y}} + R_0 \frac{\partial U_0}{\partial \breve{x}} + V_0 \frac{\partial R_0}{\partial \bar{Y}} = 0, \tag{3.3c}$$

$$H_0 = \frac{1}{(\gamma - 1) R_0}. \tag{3.3d}$$

Equations (3.3*a*,*b*) are parabolic, and require the following boundary conditions. At the leading edge of the plate, the flow is still unperturbed, and therefore we can write

$$U_0 = 1, \quad H_0 = \frac{1}{(\gamma - 1)} \quad \text{at } \breve{x} = 0, \ \ \bar{Y} \in [0, \infty). \tag{3.4a,b}$$

At the outer edge of the boundary layer, the conditions for matching of U_0 and H_0 with their values in the unperturbed flow outside the boundary layer are

$$U_0 = 1, \quad H_0 = \frac{1}{(\gamma - 1)} \quad \text{at } \bar{Y} = \infty, \ \breve{x} \in [0, \infty). \tag{3.5a,b}$$

In addition, the solution has to satisfy the no-slip conditions on the surface of the plate:

$$U_0 = V_0 = 0 \quad \text{at } \bar{Y} = 0, \ \breve{x} \in [0, \infty). \tag{3.6a}$$

These have to be supplemented with an appropriate thermal condition. Here it will be assumed that the plate is thermally isolated, in which case

$$\frac{\partial H_0}{\partial \bar{Y}} = 0 \quad \text{at } \bar{Y} = 0, \ \breve{x} \in [0, \infty). \tag{3.6b}$$

This boundary-value problem (3.3)–(3.6) admits a self-similar solution. However, for the receptivity analysis, we do not need to know the precise form of this solution. We only need to know that the solution is smooth near the position of roughness ($\breve{x} = 1$), and may be represented by the Taylor expansions

$$\left.\begin{aligned} U_0(\breve{x}, \bar{Y}) &= U_{00}(\bar{Y}) + (\breve{x} - 1)U_{01}(\bar{Y}) + \cdots, \\ R_0(\breve{x}, \bar{Y}) &= R_{00}(\bar{Y}) + (\breve{x} - 1)R_{01}(\bar{Y}) + \cdots, \\ H_0(\breve{x}, \bar{Y}) &= H_{00}(\bar{Y}) + (\breve{x} - 1)H_{01}(\bar{Y}) + \cdots, \\ \mu_0(\breve{x}, \bar{Y}) &= \mu_{00}(\bar{Y}) + (\breve{x} - 1)\mu_{01}(\bar{Y}) + \cdots, \end{aligned}\right\} \tag{3.7}$$

where $U_{00}(\bar{Y})$, $R_{00}(\bar{Y})$, $H_{00}(\bar{Y})$ and $\mu_{00}(\bar{Y})$ are such that

$$\left.\begin{aligned} U_{00}(\bar{Y}) &= \tau \bar{Y} + O(\bar{Y}^4), \\ R_{00}(\bar{Y}) &= \rho_w + O(\bar{Y}^2), \\ H_{00}(\bar{Y}) &= h_w + O(\bar{Y}^2), \\ \mu_{00}(\bar{Y}) &= \mu_w + O(\bar{Y}^2), \end{aligned}\right\} \quad \text{as } \bar{Y} \to 0, \tag{3.8a–d}$$

where τ denotes the skin friction, and h_w, μ_w and ρ_w are the enthalpy, viscosity and density on the surface of the plate, respectively. All these quantities are constants.

3.2. *Perturbations caused by acoustic noise*

We start our analysis with region 1 situated outside the boundary layer (see figure 1). We shall assume that the acoustic noise is weak, and seek the corresponding solution of the Navier–Stokes equations (2.1) in the form

$$\hat{u} = U_\infty[1 + Re^{-1/9}u_1(\tilde{t}, \bar{x})] + \cdots, \tag{3.9a}$$

$$\hat{\rho} = \rho_\infty[1 + Re^{-1/9}\rho_1(\tilde{t}, \bar{x})] + \cdots, \tag{3.9b}$$

$$\hat{p} = p_\infty + \rho_\infty U_\infty^2 Re^{-1/9}p_1(\tilde{t}, \bar{x}) + \cdots, \tag{3.9c}$$

with the independent variables $\bar{x}$ and $\tilde{t}$ given by

$$\hat{x} = L + LRe^{-2/9}\bar{x}, \quad \hat{t} = \frac{L}{U_\infty} Re^{-2/9}\tilde{t}. \tag{3.10a,b}$$

Substitution of (3.9) and (3.10) into the Navier–Stokes equation (2.1) leads to the linearised Euler equations:

$$\frac{\partial u_1}{\partial \tilde{t}} + \frac{\partial u_1}{\partial \bar{x}} = -\frac{\partial p_1}{\partial \bar{x}}, \tag{3.11a}$$

$$\frac{\partial \rho_1}{\partial \tilde{t}} + \frac{\partial \rho_1}{\partial \bar{x}} = M_\infty^2 \left(\frac{\partial p_1}{\partial \tilde{t}} + \frac{\partial p_1}{\partial \bar{x}} \right), \tag{3.11b}$$

$$\frac{\partial \rho_1}{\partial \tilde{t}} + \frac{\partial \rho_1}{\partial \bar{x}} + \frac{\partial u_1}{\partial \bar{x}} = 0. \tag{3.11c}$$

By eliminating u_1 and ρ_1, one can reduce the set of equations (3.11) to the following equation for the pressure perturbations p_1:

$$M_\infty^2 \frac{\partial^2 p_1}{\partial \tilde{t}^2} + (M_\infty^2 - 1)\frac{\partial^2 p_1}{\partial \bar{x}^2} + 2M_\infty^2 \frac{\partial^2 p_1}{\partial \bar{x}\partial \tilde{t}} = 0. \tag{3.12}$$

It admits a travelling-wave solution

$$p_a(\tilde{t}, \bar{x}) = \bar{\alpha} \sin(\tilde{\omega}\tilde{t} + \bar{k}\bar{x}), \tag{3.13}$$

where $\bar{\alpha}$ is the amplitude of the acoustic wave, $\tilde{\omega}$ is the frequency and $\bar{k} = -\tilde{\omega}M_\infty/(M_\infty + 1)$ is the wavenumber.

3.3. *Main part of the boundary layer*

The steady solution in the boundary layer is represented by the asymptotic expansions (3.1). Now we shall add the perturbations caused by the acoustic wave:

$$\hat{u} = U_\infty[U_0(\check{x}, \bar{Y}) + Re^{-1/9}M_\infty u_2(\check{x}, \bar{Y})p_a(\tilde{t}, \bar{x})] + \cdots, \tag{3.14a}$$

$$\hat{v} = U_\infty[Re^{-7/18}\bar{\alpha}\bar{k}M_\infty v_2(\check{x}, \bar{Y})\cos(\tilde{\omega}\tilde{t} + \bar{k}\bar{x})] + \cdots, \tag{3.14b}$$

$$\hat{p} = p_\infty + \rho_\infty U_\infty^2[Re^{-1/9}p_2(\check{x}, \bar{Y})p_a(\tilde{t}, \bar{x})] + \cdots, \tag{3.14c}$$

$$\hat{h} = U_\infty^2[H_0(\check{x}, \bar{Y}) + Re^{-1/9}h_2(\check{x}, \bar{Y})p_a(\tilde{t}, \bar{x})] + \cdots, \tag{3.14d}$$

$$\hat{\rho} = \rho_\infty[R_0(\check{x}, \bar{Y}) + Re^{-1/9}M_\infty^2\rho_2(\check{x}, \bar{Y})p_a(\tilde{t}, \bar{x})] + \cdots, \tag{3.14e}$$

$$\hat{\mu} = \mu_\infty[\mu_0(\check{x}, \bar{Y}) + Re^{-1/9}\mu_2(\check{x}, \bar{Y})p_a(\tilde{t}, \bar{x})] + \cdots, \tag{3.14f}$$

where the function p_a is given by (3.13), the independent variables $\tilde{t}$ and $\bar{x}$ are given by (3.10) and $\bar{Y}$ is defined by (3.2*b*).

Substituting (3.14) into (2.1) and working with the leading-order terms, we find that

$$R_0\left[\left(\frac{\tilde{\omega}}{\bar{k}} + U_0\right)u_2 + v_2\frac{\partial U_0}{\partial \bar{Y}}\right] = -\frac{p_2}{M_\infty}, \tag{3.15a}$$

$$\frac{\partial p_2}{\partial \bar{Y}} = 0, \tag{3.15b}$$

$$R_0\left[\left(\frac{\tilde{\omega}}{\bar{k}}+U_0\right)h_2+M_\infty v_2\frac{\partial H_0}{\partial \bar{Y}}\right]=\left(\frac{\tilde{\omega}}{\bar{k}}+U_0\right)p_2, \tag{3.15c}$$

$$M_\infty\left(\frac{\tilde{\omega}}{\bar{k}}+U_0\right)\rho_2+R_0u_2+\frac{\partial(v_2R_0)}{\partial \bar{Y}}=0, \tag{3.15d}$$

$$(\gamma-1)(h_2R_0+M_\infty^2\rho_2H_0)=\gamma p_2. \tag{3.15e}$$

It can be seen that these equations do not contain viscous terms. Thus, instead of the no-slip condition, the impermeability condition, $v_2=0$, on the plate surface should be applied. Consequently, setting $\bar{Y}=0$ in (3.3*a*,*c*), and choosing $\breve{x}=1$, we can find that at the bottom of the boundary layer

$$u_2=\frac{1}{\rho_w(M_\infty+1)}\quad\text{and}\quad h_2=\frac{1}{\rho_w}\quad\text{at }\bar{Y}=0. \tag{3.16a,b}$$

The solution (3.16) does not satisfy the no-slip condition, which means that we also need to consider the Stokes layer closer to the plate surface.

3.4. *Stokes layer*

As the pressure perturbations (3.13) penetrate the boundary layer, they cause the Stokes layer to form near the surface. The thickness of this layer is easily estimated by comparing the instantaneous acceleration term with the viscous forces in the longitudinal momentum equation (2.1*a*):

$$\hat{\rho}\frac{\partial\hat{u}}{\partial\hat{t}}\sim\frac{\partial}{\partial\hat{y}}\left(\hat{\mu}\frac{\partial\hat{u}}{\partial\hat{y}}\right). \tag{3.17}$$

Taking into account that $\hat{\rho}\sim\rho_\infty$, $\hat{\mu}\sim\mu_\infty$ and the characteristic time is defined by (3.10*b*), one can easily deduce from (3.17) that the thickness of the Stokes layer is $\hat{y}\sim LRe^{-11/18}$.

The solution in the Stokes layer is sought in the form

$$\left.\begin{aligned}
\hat{u}&=U_\infty Re^{-1/9}u_3(\tilde{t},\bar{x},\bar{y})+\cdots,\\
\hat{v}&=U_\infty Re^{-1/2}v_3(\tilde{t},\bar{x},\bar{y})+\cdots,\\
\hat{p}&=p_\infty+\rho_\infty U_\infty^2 Re^{-1/9}p_3(\tilde{t},\bar{x},\bar{y})+\cdots,\\
\hat{\rho}&=\rho_\infty[\rho_w+Re^{-1/9}\rho_3(\tilde{t},\bar{x},\bar{y})]+\cdots,\\
\hat{h}&=U_\infty^2[h_w+Re^{-1/9}h_3(\tilde{t},\bar{x},\bar{y})]+\cdots,\\
\hat{\mu}&=\mu_\infty[\mu_w+Re^{-1/9}\mu_3(\tilde{t},\bar{x},\bar{y})]+\cdots,
\end{aligned}\right\} \tag{3.18}$$

where $\bar{y}$ is defined by the equation

$$\hat{y}=LRe^{-11/18}\bar{y}. \tag{3.19}$$

Substituting (3.18) into the Navier–Stokes equations (2.1) and working with leading-order terms, we find that the flow in the Stokes layer is described by the equations

$$\rho_w\frac{\partial u_3}{\partial\tilde{t}}=-\frac{\partial p_3}{\partial\bar{x}}+\mu_w\frac{\partial^2u_3}{\partial\bar{y}^2}, \tag{3.20a}$$

$$\frac{\partial p_3}{\partial\bar{y}}=0, \tag{3.20b}$$

$$\rho_w \frac{\partial h_3}{\partial \tilde{t}} = \frac{\partial p_3}{\partial \tilde{t}} + \frac{\mu_w}{Pr} \frac{\partial^2 h_3}{\partial \bar{y}^2}, \tag{3.20c}$$

$$\frac{\partial \rho_3}{\partial \tilde{t}} + \rho_w \frac{\partial u_3}{\partial \bar{x}} + \rho_w \frac{\partial v_3}{\partial \bar{y}} = 0, \tag{3.20d}$$

$$(\gamma - 1)(h_w \rho_3 + \rho_w h_3) = \gamma p_3. \tag{3.20e}$$

It follows from (3.20*b*) and (3.15*b*) that the pressure does not change across the main part of the boundary layer, and it also remains unchanged across the Stokes layer. This means that p_3 is given by (3.13). With known p_3, the x momentum equation (3.20*a*) separates from the rest of the equations in (3.20). It has to be solved with the no-slip condition on the surface of the plate and the matching condition with the solution in region 2:

$$u_3 = 0 \quad \text{at } \bar{y} = 0, \tag{3.21a}$$

$$u_3 = \tau \bar{y} - \frac{\bar{k}}{\tilde{\omega}} \frac{p_a}{\rho_w} \quad \text{as } \bar{y} \to \infty. \tag{3.21b}$$

The solution of the boundary-value problem (3.20*a*) and (3.21) is written as

$$u_3 = \tau \bar{y} + d \sin(\tilde{\omega}\tilde{t} + \bar{k}\bar{x}) - d\mathrm{e}^{-\chi \bar{y}} \sin(\tilde{\omega}\tilde{t} + \bar{k}\bar{x} - \chi \bar{y}), \tag{3.22}$$

where

$$d = -\frac{\bar{k}\bar{\alpha}}{\tilde{\omega}\rho_w}, \quad \chi = \sqrt{\frac{\tilde{\omega}\rho_w}{2\mu_w}}. \tag{3.23a,b}$$

4. Flow in the interaction region

As was stated in the introduction, for effective generation of the Tollmien–Schlichting waves, the Stokes layer has to come into interaction with the wall roughness (see figure 2). To satisfy the resonance conditions, we shall assume that the longitudinal size of the roughness is estimated as

$$\Delta \hat{x} = O(LRe^{-1/3}), \tag{4.1}$$

i.e. is comparable with the wavelength of the Tollmien–Schlichting wave. Keeping this in mind, we shall express the roughness shape by the equation

$$\hat{y} = LRe^{-11/18} \bar{G}\left(\frac{\hat{x} - L}{LRe^{-3/9}}\right). \tag{4.2}$$

The triple-deck region that forms in the vicinity of the roughness is composed of three tiers: the viscous sublayer of thickness $\hat{y} \sim LRe^{-11/18}$, the main part of the boundary layer with thickness $\hat{y} \sim LRe^{-1/2}$, and the potential flow region that lies outside the boundary layer; the thickness of the upper tier is estimated as $\hat{y} \sim LRe^{-5/18}$. Of course, all three layers have the same longitudinal extent given by (4.1). Correspondingly, an order-one longitudinal coordinate for the triple-deck region, $\tilde{x}$, is introduced as

$$\hat{x} = L + LRe^{-1/3}\tilde{x}. \tag{4.3}$$

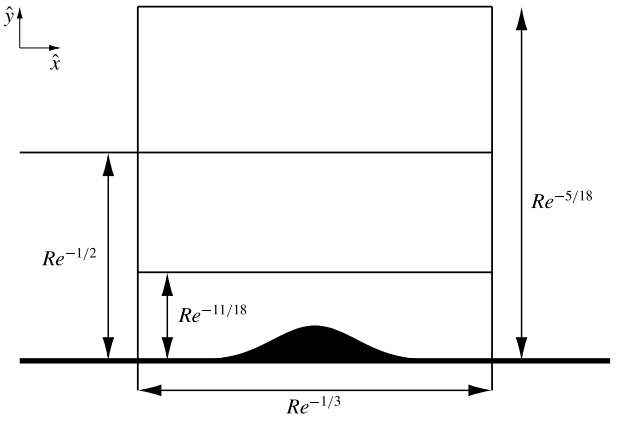

FIGURE 2. Triple-deck structure in transonic flow.

Before analysing the flow behaviour in the three tiers, we shall make the following observation. The size of the roughness is much smaller than the wavelength of the acoustic wave. Indeed, comparing (4.3) with (3.10*a*), we can see that

$$\bar{x} = Re^{-1/9}\tilde{x}. \tag{4.4}$$

Substituting (4.4) into (3.13) and setting $Re \to \infty$ with $\tilde{x} = O(1)$, we find that, in the interaction region, the acoustic pressure perturbations may be expressed by the equation

$$p_a = \bar{\alpha}\sin(\tilde{\omega}\tilde{t}) + Re^{-1/9}\bar{\alpha}\bar{k}\tilde{x}\cos(\tilde{\omega}\tilde{t}) + \cdots. \tag{4.5}$$

4.1. *Lower deck*

We start the analysis of the flow in the interaction region with the viscous near-wall layer, shown as region 4 in figure 1. The characteristic thickness of region 4 is the same as that of the Stokes layer (region 3). Keeping in mind that the solution in the Stokes layer is represented by asymptotic expansions (3.18), we seek the solution of the Navier–Stokes equations in region 4 in the form

$$\left.\begin{gathered} \hat{u} = U_\infty Re^{-1/9}u_4(\tilde{t},\tilde{x},\bar{y}) + \cdots, \quad \hat{v} = U_\infty Re^{-7/18}v_4(\tilde{t},\tilde{x},\bar{y}) + \cdots, \\ \hat{p} = p_\infty + \rho_\infty U_\infty^2\{Re^{-1/9}\bar{\alpha}\sin(\tilde{\omega}\tilde{t}) + Re^{-2/9}[p_4(\tilde{t},\tilde{x},\bar{y}) + \bar{\alpha}\bar{k}\tilde{x}\cos(\tilde{\omega}\tilde{t})]\} + \cdots, \\ \hat{\rho} = \rho_\infty\rho_w + \cdots, \quad \hat{\mu} = \mu_\infty\mu_w + \cdots, \quad \hat{h} = h_\infty h_w + \cdots, \end{gathered}\right\} \tag{4.6}$$

with independent variables $\tilde{t}$, $\tilde{x}$ and $\tilde{y}$ defined by

$$\hat{t} = \frac{L}{U_\infty}Re^{-2/9}\tilde{t}, \quad \hat{x} = L + LRe^{-1/3}\tilde{x}, \quad \hat{y} = LRe^{-11/18}\bar{y}. \tag{4.7a–c}$$

Substitution of (4.6) and (4.7) into the Navier–Stokes equations (2.1) shows that pressure p_4 does not change across region 4, and the momentum (2.1*a*) and continuity (2.1*d*) equations assume the form

$$\rho_w\left(\frac{\partial u_4}{\partial \tilde{t}}+u_4\frac{\partial u_4}{\partial \tilde{x}}+v_4\frac{\partial u_4}{\partial \bar{y}}\right)=\bar{\alpha}\bar{k}\cos(\tilde{\omega}\tilde{t})-\frac{\partial p_4}{\partial \tilde{x}}+\mu_w\frac{\partial^2 u_4}{\partial \bar{y}^2}, \tag{4.8a}$$

$$\frac{\partial u_4}{\partial \tilde{x}}+\frac{\partial v_4}{\partial \bar{y}}=0, \tag{4.8b}$$

and decouple from the rest of the equations.

Equations (4.8) have to be solved with the no-slip conditions on the surface of the roughness,

$$u_4=v_4=0 \quad \text{at } \bar{y}=\bar{G}(\tilde{x}), \tag{4.9a}$$

and match with the solution (3.22) in the Stokes layer (region 3),

$$u_4=\tau\bar{y}+d\sin(\tilde{\omega}\tilde{t})-de^{-\chi\bar{y}}\sin(\tilde{\omega}\tilde{t}-\chi\bar{y}) \quad \text{as } \tilde{x}\to-\infty. \tag{4.9b}$$

4.2. *Middle deck*

The flow in the middle deck (region 5 in figure 1) displays its usual behaviour. Owing to higher fluid velocity, this region is less sensitive to the pressure perturbation than the viscous sublayer. As a consequence, the middle deck does not contribute to the displacement effect of the boundary layer. Instead, it simply 'transmits' the deformations of the streamlines, produced in the viscous sublayer, to the upper deck. The solution in region 5 is constructed in the same way as was done for the corresponding subsonic flow (see Ruban 1984). We found that

$$\hat{u}=U_\infty\left\{U_{00}(\bar{Y})+Re^{-1/9}\left[M_\infty\bar{\alpha}u_2(1,\bar{Y})\sin(\tilde{\omega}\tilde{t})+A_*(\tilde{t},\tilde{x})\frac{\mathrm{d}U_{00}}{\mathrm{d}\bar{Y}}(\bar{Y})\right]\right\}+\cdots, \tag{4.10a}$$

$$\hat{v}=-U_\infty Re^{-5/18}U_{00}(\bar{Y})\frac{\partial A_*}{\partial \tilde{x}}(\tilde{t},\tilde{x})+\cdots, \tag{4.10b}$$

$$\hat{p}=p_\infty+\rho_\infty U_\infty^2\{Re^{-1/9}\bar{\alpha}\sin(\tilde{\omega}\tilde{t})+Re^{-2/9}[p_5(\tilde{t},\tilde{x})+\bar{\alpha}\bar{k}\tilde{x}\cos(\tilde{\omega}\tilde{t})]\}+\cdots, \tag{4.10c}$$

$$\hat{\rho}=\rho_\infty\left\{R_{00}(\bar{Y})+Re^{-1/9}\left[M_\infty^2\bar{\alpha}\rho_2(1,\bar{Y})\sin(\tilde{\omega}\tilde{t})+A_*(\tilde{t},\tilde{x})\frac{\mathrm{d}R_{00}}{\mathrm{d}\bar{Y}}(\bar{Y})\right]\right\}+\cdots. \tag{4.10d}$$

Here $A_*(\tilde{t},\tilde{x})$ is the displacement function. It is not known at this stage of the analysis, and has to be found together with the pressure perturbation function p_5. The latter does not change across this region, and therefore coincides with corresponding function p_4 in the viscous sublayer.

For future use we need to mention that matching of (4.10*a*) with the asymptotic expansion for $\hat{u}$ in (4.6) shows that the solution of equations (4.8) should satisfy the following boundary condition at the outer edge of the viscous sublayer layer (region 4):

$$u_4=\tau[\bar{y}+A_*(\tilde{t},\tilde{x})]-\frac{\bar{k}}{\tilde{\omega}}\frac{\bar{\alpha}}{\rho_w}\sin(\tilde{\omega}\tilde{t}) \quad \text{as } \bar{y}\to\infty. \tag{4.11}$$

We also need to perform the matching with the solution in the upper tier (region 6 in figure 1). Setting $\bar{Y}\to\infty$ in (4.10*b*) and taking into account that $U_{00}(\infty)=1$, we find that at the 'bottom' of region 6

$$\hat{v}=-U_\infty Re^{-5/18}\frac{\partial A_*}{\partial \tilde{x}}. \tag{4.12}$$

4.3. *Upper deck*

Guided by (4.12) we represent the pressure in region 6 in the form of the asymptotic expansion

$$\hat{p} = p_\infty + \rho_\infty U_\infty^2 \{Re^{-1/9}\bar{\alpha}\sin(\tilde{\omega}\tilde{t}) + Re^{-2/9}[p_6(\tilde{t},\tilde{x},\tilde{y}) + \bar{\alpha}\bar{k}\tilde{x}\cos(\tilde{\omega}\tilde{t})]\} + \cdots, \quad (4.13)$$

with the independent variables scaled as

$$\hat{t} = \frac{L}{U_\infty} Re^{-2/9}\tilde{t}, \quad \hat{x} = L + LRe^{-1/3}\tilde{x}, \quad \hat{y} = LRe^{-5/18}\tilde{y}. \quad (4.14a\text{–}c)$$

The equation for the pressure perturbation function p_6 was deduced by Timoshin (1990). It has the form

$$2\frac{\partial^2 p_6}{\partial\tilde{x}\partial\tilde{t}} + Q_\infty \frac{\partial^2 p_6}{\partial\tilde{x}^2} - \frac{\partial^2 p_6}{\partial\tilde{y}^2} = 0, \quad (4.15)$$

where Q_∞ is defined by (2.5). Note that, in contrast to what happens in subsonic and supersonic flows, equation (4.15) retains the time derivative and is hyperbolic if $Q_\infty > 0$, and elliptic otherwise.

Equation (4.15) requires two boundary conditions. The first is the matching condition with the solution (4.12) in the middle tier. When written for the pressure perturbation function p_6 it has the form

$$\frac{\partial p_6}{\partial\tilde{y}} = \frac{\partial^2 A_*}{\partial\tilde{x}^2} \quad \text{at } \tilde{y} = 0. \quad (4.16a)$$

The second condition depends on the perturbation mode considered. If it is 'subsonic', then we will use the attenuation condition

$$p_6 \to 0 \quad \text{as } \tilde{y} \to \infty. \quad (4.16b)$$

If the flow regime is 'supersonic', then (4.16*b*) will be substituted by a causality rule.

4.4. *Viscous–inviscid interaction problem*

When dealing with the interaction region, one has to solve equations (4.8) in the viscous sublayer simultaneously with (4.15) in the upper deck. The solution to equations (4.8) has to be found subject to the boundary conditions (4.9) and (4.11), while (4.15) has to be solved with the boundary condition (4.16) or its 'supersonic' counterpart. Considered together, these equations and boundary conditions constitute the viscous–inviscid interaction problem. To reduce the number of parameters involved, we shall perform the following affine transformation of the variables in the viscous sublayer:

$$\left.\begin{aligned} \tilde{t} = (\rho_w\mu_w^{-5}\tau^{-14})^{1/9}t, \quad \tilde{x} = (\rho_w^{-3}\mu_w^{-3}\tau^{-12})^{1/9}x, \\ \bar{y} = (\rho_w^{-4}\mu_w^2\tau^{-7})^{1/9}[y + g(x)], \quad p_4 = (\rho_w\mu_w^4\tau^4)^{1/9}p, \\ u_4 = (\rho_w^{-4}\mu_w^2\tau^2)^{1/9}u, \quad v_4 = (\rho_w^{-5}\mu_w^7\tau^7)^{1/9}\left[v + u\frac{\mathrm{d}g}{\mathrm{d}x}\right], \\ A_* = (\rho_w^{-4}\mu_w^2\tau^{-7})^{1/9}[A - g(x)], \quad \bar{G} = (\rho_w^{-4}\mu_w^2\tau^{-7})^{1/9}g(x). \end{aligned}\right\} \quad (4.17)$$

Notice that, in addition to affine transformations, the above equations also include (in square brackets) the Prandtl transposition theorem.

The frequency and amplitude of the acoustic perturbation are scaled as

$$\tilde{\omega} = (\rho_w^{-1}\mu_w^5\tau^{14})^{1/9}\omega, \quad \bar{\alpha} = \frac{(\rho_w^4\mu_w^7\tau^{16})^{1/9}}{\bar{k}}\alpha. \tag{4.18a,b}$$

Correspondingly, for the upper deck we introduce the following transformations:

$$p_6 = (\rho_w\mu_w^4\tau^4)^{1/9}P, \quad \tilde{y} = (\rho_w^{-1}\mu_w^{-4}\tau^{-13})^{1/9}Y. \tag{4.19a,b}$$

Finally, the Kármán–Guderley parameter is transformed as

$$Q_\infty = (\rho_w^{-4}\mu_w^2\tau^2)^{1/9}K_\infty. \tag{4.20}$$

As a result the lower-deck equations (4.8) assume the form

$$\frac{\partial u}{\partial t} + u\frac{\partial u}{\partial x} + v\frac{\partial u}{\partial y} = \alpha\cos(\omega t) - \frac{\partial p}{\partial x} + \frac{\partial^2 u}{\partial y^2}, \tag{4.21a}$$

$$\frac{\partial u}{\partial x} + \frac{\partial v}{\partial y} = 0, \tag{4.21b}$$

with boundary conditions (4.9) and (4.11) turning into

$$u = v = 0 \quad \text{at } y = 0, \tag{4.22a}$$

$$u = y - \frac{\alpha}{\omega}\left[\sin(\omega t) - \mathrm{e}^{-\sqrt{\omega/2}y}\sin\left(\omega t - \sqrt{\frac{\omega}{2}}y\right)\right] \quad \text{as } x \to -\infty, \tag{4.22b}$$

$$u = y + A - \frac{\alpha}{\omega}\sin(\omega t) \quad \text{as } y \to \infty. \tag{4.22c}$$

The upper-deck equation (4.15) is now written as

$$2\frac{\partial^2 P}{\partial x \partial t} + K_\infty\frac{\partial^2 P}{\partial x^2} - \frac{\partial^2 P}{\partial Y^2} = 0, \tag{4.23}$$

and the boundary conditions (4.16) assume the form

$$\frac{\partial P}{\partial Y} = \frac{\partial^2 A}{\partial x^2} - \frac{\partial^2 g}{\partial x^2} \quad \text{at } Y = 0, \tag{4.24a}$$

$$P \to 0 \quad \text{as } Y \to \infty. \tag{4.24b}$$

The statement that the pressure at the 'bottom' of region 6 coincides with the pressure in region 4,

$$P|_{Y=0} = p, \tag{4.25}$$

closes the viscous–inviscid interaction problem.

5. Linear receptivity

Here we shall assume that the amplitude of the acoustic wave, α, is small, and the wall roughness is 'shallow', namely, we shall write the roughness equation in the form

$$y = g(x) = hF(x), \tag{5.1}$$

and apply to the interaction problem (4.21)–(4.25) the limit procedure

$$\alpha \to 0, \quad h \to 0. \tag{5.2a,b}$$

The asymptotic solution in the lower deck is sought in the form

$$u = y + \alpha U_s(t, y) + hu_r(x, y) + \alpha hu'(t, x, y) + \cdots, \tag{5.3a}$$

$$v = hv_r(x, y) + \alpha hv'(t, x, y) + \cdots, \tag{5.3b}$$

$$p = \alpha \sin(\omega t) + hp_r(x, y) + \alpha hp'(t, x, y) + \cdots, \tag{5.3c}$$

$$A = hA_r(x, y) + \alpha hA'(t, x, y) + \cdots. \tag{5.3d}$$

In the asymptotic expansion for u, the leading-order term, $u = y$, represents the unperturbed steady boundary layer, and would be the only term if neither the Stokes layer nor roughness were present. The next term, $\alpha U_s(t, y)$ with

$$U_s(t, y) = -\frac{1}{\omega}\left[\sin(\omega t) - \mathrm{e}^{-\sqrt{\omega/2}y} \sin\left(\omega t - \sqrt{\frac{\omega}{2}}y\right)\right], \tag{5.4}$$

represents the perturbations produced by the Stokes layer. The third term, $hu_r(x, y)$, stands for the steady perturbations produced by the wall roughness. Finally, the fourth term, $\alpha hu'(t, x, y)$, represents the perturbations produced in the boundary layer due to the interaction of the Stokes layer with the steady flow field around the roughness.

Corresponding to (5.3), the solution in the upper deck is represented as

$$P = \alpha \sin(\omega t) + hP_r(x, Y) + \alpha hP'(t, x) + \cdots. \tag{5.5}$$

We start with the analysis of steady perturbations produced by the roughness.

5.1. *Steady problem*

Substituting (5.3) into (4.21) and (4.22), and working with $O(h)$ terms, we find that, in the viscous sublayer, the steady perturbations are described by the equations

$$\frac{\partial u_r}{\partial x} + \frac{\partial v_r}{\partial y} = 0, \tag{5.6a}$$

$$y\frac{\partial u_r}{\partial x} + v_r = -\frac{\partial p_r}{\partial x} + \frac{\partial^2 u_r}{\partial y^2}, \tag{5.6b}$$

which have to be solved with the boundary conditions

$$u_r = v_r = 0 \quad \text{at } y = 0, \tag{5.7a}$$

$$u_r = A_r \quad \text{as } y \to \infty, \tag{5.7b}$$

$$u_r = 0 \quad \text{as } x \to -\infty. \tag{5.7c}$$

Similarly, substitution of (5.5) into (4.23) and (4.20) results in

$$K_\infty \frac{\partial^2 P_r}{\partial x^2} - \frac{\partial^2 P_r}{\partial Y^2} = 0, \tag{5.8a}$$

$$\frac{\partial P_r}{\partial Y} = \frac{\partial^2 A_r}{\partial x^2} - \frac{\partial^2 F}{\partial x^2} \quad \text{at } Y = 0, \tag{5.8b}$$

$$P_r \to 0 \quad \text{as } Y \to \infty. \tag{5.8c}$$

The solution of the problem (5.6)–(5.8) may be constructed in the same way as was done with the problem (4.14) and (4.15) in Ruban *et al.* (2013). The main difference is that now (5.8*a*) changes its type from elliptic in subsonic flow ($K_\infty < 0$) to hyperbolic in supersonic flow ($K_\infty > 0$). In the latter case, the condition (5.8*c*) has to be relaxed and substituted by the 'causality condition', according to which the perturbations produced by the roughness can only propagate downstream. As in Ruban *et al.* (2013) we apply the Fourier transform to equation (5.8*a*). With the Fourier transform of $P_r(x, Y)$ defined as

$$\bar{P}_r(k, Y) = \int_{-\infty}^{\infty} P_r(x, Y) \mathrm{e}^{-\mathrm{i}kx}\, \mathrm{d}x, \tag{5.9}$$

we have

$$k^2 |K_\infty| \bar{P}_r - \frac{\mathrm{d}^2 \bar{P}_r}{\mathrm{d}Y^2} = 0 \quad \text{if } K_\infty < 0, \tag{5.10a}$$

$$k^2 |K_\infty| \bar{P}_r + \frac{\mathrm{d}^2 \bar{P}_r}{\mathrm{d}Y^2} = 0 \quad \text{if } K_\infty > 0. \tag{5.10b}$$

The boundary condition (5.8*b*) is written in terms of Fourier transforms as

$$\frac{\mathrm{d}\bar{P}_r}{\mathrm{d}Y} = -k^2(\bar{A}_r - \bar{F}) \quad \text{at } Y = 0. \tag{5.11}$$

The solution to (5.10) and (5.11) satisfying the disturbance attenuation condition for $K_\infty < 0$, and the causality condition for $K_\infty > 0$, has the form

$$\bar{P}_r = \mathrm{i}|k|(\bar{A}_r - \bar{F})\varkappa^{-1}|K_\infty|^{-1/2} \mathrm{e}^{\mathrm{i}|k|\varkappa\sqrt{|K_\infty|}Y}, \tag{5.12}$$

where

$$\varkappa = \begin{cases} \mathrm{i} & \text{if } K_\infty < 0, \\ -1 & \text{if } K_\infty > 0. \end{cases} \tag{5.13}$$

The solution of the boundary-value problem (5.6) and (5.7) for the viscous sublayer can now be found in the usual way (see e.g. Ruban *et al.* 2013). We have

$$\bar{u}_r = \bar{F}(k)\Phi(z; k, K_\infty) \quad \text{and} \quad \bar{v}_r = \bar{F}(k)\Psi(z; k, K_\infty), \tag{5.14a,b}$$

where $z = (\mathrm{i}k)^{1/3} y$, $\bar{F}$ is the Fourier transform of the roughness shape function $F(x)$, and

$$\Phi(z; k, K_\infty) = \frac{3\mathrm{i}(\mathrm{i}k)^{1/3}|k|}{\mathrm{i}(\mathrm{i}k)^{1/3}|k| - 3\varkappa \mathrm{Ai}'(0)|K_\infty|^{1/2}} \int_0^z \mathrm{Ai}(s)\, \mathrm{d}s, \tag{5.15a}$$

$$\Psi(z; k, K_\infty) = -(\mathrm{i}k)^{2/3} \int_0^z \Phi(s; k, K_\infty)\, \mathrm{d}s. \tag{5.15b}$$

Remember that the analytic branch of $(\mathrm{i}k)^{1/3}$ is chosen by making a branch cut in the complex k-plane along the positive imaginary semi-axis.

5.2. *Unsteady problem*

When dealing with the $O(\alpha h)$ terms in (5.3) and (5.5), we have to solve the following equations in the viscous sublayer:

$$\left.\begin{gathered}\frac{\partial u'}{\partial t}+y\frac{\partial u'}{\partial x}+v'+U_s\frac{\partial u_r}{\partial x}+v_r\frac{\partial U_s}{\partial y}=-\frac{\partial p'}{\partial x}+\frac{\partial^2 u'}{\partial y^2},\\ \frac{\partial u'}{\partial x}+\frac{\partial v'}{\partial y}=0.\end{gathered}\right\} \tag{5.16}$$

The boundary conditions for (5.16) are

$$\left.\begin{aligned}&u'=v'=0 \quad \text{at } y=0,\\ &u'=A' \quad \text{as } y\to\infty,\\ &u'=0 \quad \text{as } x\to-\infty.\end{aligned}\right\} \tag{5.17}$$

In the upper deck the pressure perturbations are described by the equation

$$2\frac{\partial^2 P'}{\partial x\partial t}+K_\infty\frac{\partial^2 P'}{\partial x^2}-\frac{\partial^2 P'}{\partial Y^2}=0. \tag{5.18}$$

This has to be solved with the boundary conditions

$$\left.\begin{aligned}&\frac{\partial P'}{\partial Y}=\frac{\partial^2 A'}{\partial x^2} \quad \text{at } Y=0,\\ &P'\to 0 \quad \text{as } Y\to\infty.\end{aligned}\right\} \tag{5.19}$$

The solution of the boundary-value problem (5.16)–(5.19) is sought in the time-periodic form:

$$(u',\,v',\,p',\,P',\,A',\,U_s)=(\tilde{u},\,\tilde{v},\,\tilde{p},\,\tilde{P},\,\tilde{A},\,\tilde{U}_s)\mathrm{e}^{\mathrm{i}\omega t}+\text{c.c.}, \tag{5.20}$$

where c.c. denotes the complex conjugate, and

$$\tilde{U}_s=\frac{\mathrm{i}}{2\omega}[1-\mathrm{e}^{-(\mathrm{i}+1)\sqrt{\omega/2}y}]. \tag{5.21}$$

Substitution of (5.20) and (5.21) into (5.16) and (5.17) turns the boundary-value problem for the viscous sublayer into

$$\left.\begin{gathered}\mathrm{i}\omega\tilde{u}+y\frac{\partial\tilde{u}}{\partial x}+\tilde{v}+\tilde{U}_s\frac{\partial u_r}{\partial x}+v_r\frac{\partial\tilde{U}_s}{\partial y}=-\frac{\partial\tilde{p}}{\partial x}+\frac{\partial^2\tilde{u}}{\partial y^2},\\ \frac{\partial\tilde{u}}{\partial x}+\frac{\partial\tilde{v}}{\partial y}=0,\\ \tilde{u}=\tilde{v}=0 \quad \text{at } y=0,\\ \tilde{u}=\tilde{A} \quad \text{as } y\to\infty,\\ \tilde{u}=0 \quad \text{as } x\to-\infty.\end{gathered}\right\} \tag{5.22}$$

Similarly, the upper-deck boundary-value problem (5.18) and (5.19) takes the form

$$2\mathrm{i}\omega\frac{\partial\tilde{P}}{\partial x}+K_\infty\frac{\partial^2\tilde{P}}{\partial x^2}-\frac{\partial^2\tilde{P}}{\partial Y^2}=0, \tag{5.23a}$$

$$\frac{\partial \tilde{P}}{\partial Y} = \frac{\partial^2 \tilde{A}}{\partial x^2} \quad \text{at } Y = 0, \tag{5.23b}$$

$$\tilde{P} \to 0 \quad \text{as } Y \to \infty. \tag{5.23c}$$

Applying the Fourier transform to (5.23*a*,*b*), we have

$$\left.\begin{aligned} \frac{\mathrm{d}^2 \check{P}}{\mathrm{d}Y^2} + (2\omega k + k^2 K_\infty)\check{P} = 0, \\ \frac{\mathrm{d}\check{P}}{\mathrm{d}Y} = -k^2 \check{A} \quad \text{at } Y = 0. \end{aligned}\right\} \tag{5.24}$$

Here $\check{P}$ is the Fourier transform of $\tilde{P}$, and $\check{A}$ is the Fourier transform of $\tilde{A}$. The solution to (5.24) satisfying the attenuation/causality conditions at large Y is written as

$$\check{P} = \mathrm{i}k^2 \check{A} \sigma^{-1} \mathrm{e}^{\mathrm{i}\sigma Y}. \tag{5.25}$$

Here σ is calculated for subsonic flow ($K_\infty < 0$) as

$$\sigma = \begin{cases} -\sqrt{2\omega k - k^2 |K_\infty|} & \text{for } k \in \left[0, \dfrac{2\omega}{|K_\infty|}\right], \\ \mathrm{i}\sqrt{-2\omega k + k^2 |K_\infty|} & \text{for } k \in (-\infty, 0) \cup \left(\dfrac{2\omega}{|K_\infty|}, \infty\right), \end{cases} \tag{5.26}$$

and for the supersonic flow ($K_\infty > 0$) as

$$\sigma = \begin{cases} \sqrt{-2\omega |k| + k^2 K_\infty} & \text{for } k \in \left(-\infty, -\dfrac{2\omega}{|K_\infty|}\right), \\ \mathrm{i}\sqrt{2\omega |k| - k^2 K_\infty} & \text{for } k \in \left[-\dfrac{2\omega}{|K_\infty|}, 0\right], \\ -\sqrt{2\omega k + k^2 K_\infty} & \text{for } k \in (0, \infty). \end{cases} \tag{5.27}$$

Setting $Y = 0$ in (5.25) gives the Fourier transform of the pressure in the viscous sublayer:

$$\check{p} = \mathrm{i}k^2 \check{A} \sigma^{-1}. \tag{5.28}$$

The boundary-value problem (5.22) for the viscous sublayer is written in terms of the Fourier transforms as

$$\mathrm{i}\omega \check{u} + \mathrm{i}ky\check{u} + \check{v} + \mathrm{i}k\tilde{U}_s \bar{u}_r + \bar{v}_r \frac{\mathrm{d}\tilde{U}_s}{\mathrm{d}y} = -\mathrm{i}k\check{p} + \frac{\mathrm{d}^2 \check{u}}{\mathrm{d}y^2}, \tag{5.29a}$$

$$\mathrm{i}k\check{u} + \frac{\mathrm{d}\check{v}}{\mathrm{d}y} = 0, \tag{5.29b}$$

$$\check{u} = \check{v} = 0 \quad \text{at } y = 0, \tag{5.29c}$$

$$\check{u} = \check{A} \quad \text{at } y = \infty. \tag{5.29d}$$

Differentiating (5.29*a*) with respect to y, and eliminating $\mathrm{d}\check{v}/\mathrm{d}y$ with the help of (5.29*b*), we find that

$$\mathrm{i}(ky + \omega)\frac{\mathrm{d}\check{u}}{\mathrm{d}y} + \mathrm{i}k\tilde{U}_s \frac{\mathrm{d}\bar{u}_r}{\mathrm{d}y} + \bar{v}_r \frac{\mathrm{d}^2 \tilde{U}_s}{\mathrm{d}y^2} = \frac{\mathrm{d}^3 \check{u}}{\mathrm{d}y^3}. \tag{5.30}$$

This equation has to be solved with the boundary conditions

$$\check{u} = 0 \quad \text{at } y = 0, \tag{5.31a}$$

$$\check{u} = \check{A} \quad \text{as } y \to \infty. \tag{5.31b}$$

$$\frac{\mathrm{d}^2\check{u}}{\mathrm{d}y^2} = \mathrm{i}k\check{p} = -k^3\check{A}\sigma^{-1} \quad \text{at } y = 0. \tag{5.31c}$$

The third boundary condition has been obtained by setting $y = 0$ in (5.29*a*) and using (5.28).

Equations (5.14) suggest that the solution of the boundary-value problem (5.30) and (5.31) may be represented as

$$\check{u} = \bar{F}(k)\bar{\bar{u}}, \quad \check{A} = \bar{F}(k)\bar{\bar{A}}. \tag{5.32a,b}$$

Introducing a new independent variable

$$\zeta = (\mathrm{i}k)^{1/3}y + \zeta_0, \tag{5.33}$$

where $\zeta_0 = \mathrm{i}\omega/(\mathrm{i}k)^{2/3}$, it is easily shown that $\mathrm{d}\bar{\bar{u}}/\mathrm{d}\zeta$ satisfies the inhomogeneous Airy equation:

$$\frac{\mathrm{d}^3\bar{\bar{u}}}{\mathrm{d}\zeta^3} - \zeta\frac{\mathrm{d}\bar{\bar{u}}}{\mathrm{d}\zeta} = \bar{\bar{H}}(\zeta; k, \omega, K_\infty), \tag{5.34}$$

with

$$\bar{\bar{H}}(\zeta; k, \omega, K_\infty) = (\mathrm{i}k)^{1/3}\tilde{U}_s\frac{\mathrm{d}\Phi}{\mathrm{d}z} + (\mathrm{i}k)^{-1}\frac{\mathrm{d}^2\tilde{U}_s}{\mathrm{d}y^2}\Psi. \tag{5.35}$$

This should be solved subject to the following boundary conditions:

$$\bar{\bar{u}} = 0 \quad \text{at } \zeta = \zeta_0, \tag{5.36a}$$

$$\frac{\mathrm{d}^2\bar{\bar{u}}}{\mathrm{d}\zeta^2} = \mathrm{i}(\mathrm{i}k)^{1/3}k^2\bar{\bar{A}}\sigma^{-1} \quad \text{as } \zeta = \zeta_0, \tag{5.36b}$$

$$\bar{\bar{u}} = \bar{\bar{A}} \quad \text{as } \zeta \to \infty. \tag{5.36c}$$

The general solution of (5.34) is a composition of two complementary solutions of the Airy equation and a particular integral:

$$\frac{\mathrm{d}\bar{\bar{u}}}{\mathrm{d}\zeta} = C_1\mathrm{Ai}(\zeta) + C_2\mathrm{Bi}(\zeta) + \varphi(\zeta). \tag{5.37}$$

Here we choose $\varphi(\zeta)$ to be the solution to the following boundary-value problem:

$$\varphi'' - \zeta\varphi = \bar{\bar{H}}, \tag{5.38a}$$

$$\varphi'(\zeta_0) = 0, \tag{5.38b}$$

$$\varphi(\infty) = 0. \tag{5.38c}$$

To avoid exponential growth of $\mathrm{d}\bar{\bar{u}}/\mathrm{d}\zeta$ as $\zeta \to \infty$, we set $C_2 = 0$ in (5.37). Thus, we have

$$\frac{\mathrm{d}\bar{\bar{u}}}{\mathrm{d}\zeta} = C_1\mathrm{Ai}(\zeta) + \varphi(\zeta). \tag{5.39}$$

Then, applying boundary conditions (5.36), we obtain two equations for the constant C_1 and the displacement function $\bar{\bar{A}}$:

$$C_1\mathrm{Ai}'(\zeta_0) = \mathrm{i}(\mathrm{i}k)^{1/3}k^2\bar{\bar{A}}\sigma^{-1}, \quad C_1\int_{\zeta_0}^{\infty}\mathrm{Ai}(s)\,\mathrm{d}s + \int_{\zeta_0}^{\infty}\varphi(s)\,\mathrm{d}s = \bar{\bar{A}}. \tag{5.40a,b}$$

Eliminating C_1 from (5.40), we find that

$$\bar{\bar{A}} = \frac{\mathrm{Ai}'(\zeta_0)\displaystyle\int_{\zeta_0}^{\infty}\varphi(s)\,\mathrm{d}s}{\mathrm{Ai}'(\zeta_0) - \mathrm{i}(\mathrm{i}k)^{1/3}k^2\sigma^{-1}\displaystyle\int_{\zeta_0}^{\infty}\mathrm{Ai}(s)\,\mathrm{d}s}. \tag{5.41}$$

Finally, we substitute (5.41) into (5.31*b*) and then into (5.28). We find that the Fourier transform of the pressure is given by

$$\check{p} = \frac{\mathrm{i}k^2\mathrm{Ai}'(\zeta_0)\bar{F}(k)\displaystyle\int_{\zeta_0}^{\infty}\varphi(s)\,\mathrm{d}s}{\sigma\mathrm{Ai}'(\zeta_0) - \mathrm{i}(\mathrm{i}k)^{1/3}k^2\displaystyle\int_{\zeta_0}^{\infty}\mathrm{Ai}(s)\,\mathrm{d}s}. \tag{5.42}$$

To return to physical variables, one needs to apply the inverse Fourier transform to (5.42):

$$P(t,x) = \frac{\mathrm{e}^{\mathrm{i}\omega t}}{2\pi}\int_{-\infty}^{\infty}\frac{\mathrm{i}k^2\mathrm{Ai}'(\zeta_0)\displaystyle\int_{\zeta_0}^{\infty}\varphi(s)\,\mathrm{d}s}{\sigma\mathrm{Ai}'(\zeta_0) - \mathrm{i}(\mathrm{i}k)^{1/3}k^2\displaystyle\int_{\zeta_0}^{\infty}\mathrm{Ai}(s)\,\mathrm{d}s}\bar{F}(k)\mathrm{e}^{\mathrm{i}kx}\,\mathrm{d}k. \tag{5.43}$$

Here the integration is performed along the real axis in the k-plane. For our purposes, it is convenient to take the analytic extension of the integrand into the complex k-plane, and deform the contour of integration. When performing this task, one needs to know the singularities of the integrand. Setting the denominator in (5.43) to zero results in the following dispersion relation:

$$\sigma\mathrm{Ai}'(\zeta_0) - \mathrm{i}(\mathrm{i}k)^{1/3}k^2\int_{\zeta_0}^{\infty}\mathrm{Ai}(s)\,\mathrm{d}s = 0, \tag{5.44}$$

with σ and ζ_0 defined as in (5.26), (5.27) and (5.33).

When solving (5.44) we will assume that the frequency, ω, is real and positive. Our task will be to find the wavenumber, k, which in the general case is complex and is a function of ω and K_∞. We expect the Tollmien–Schlichting waves to propagate downstream, which happens when the real part of the wavenumber is negative. Also, when solving the dispersion equation (5.44), it should be remembered that the real part of $\sqrt{2\omega k + k^2K_\infty}$ has been assumed positive in (5.26) and (5.27). We start the calculations by assuming that $\omega \to 0$ and ζ_0 is finite, which consequently leads to the limit $k \to 0$. In addition, it can be deduced from (5.33) that ω is an $O(k^{2/3})$ quantity and thus $\sigma = O(k)$. Taking these into account, we can see that the dispersion equation (5.44) reduces to

$$\frac{\mathrm{dAi}(\zeta)}{\mathrm{d}\zeta} = 0 \quad \text{at } \zeta = \zeta_0. \tag{5.45}$$

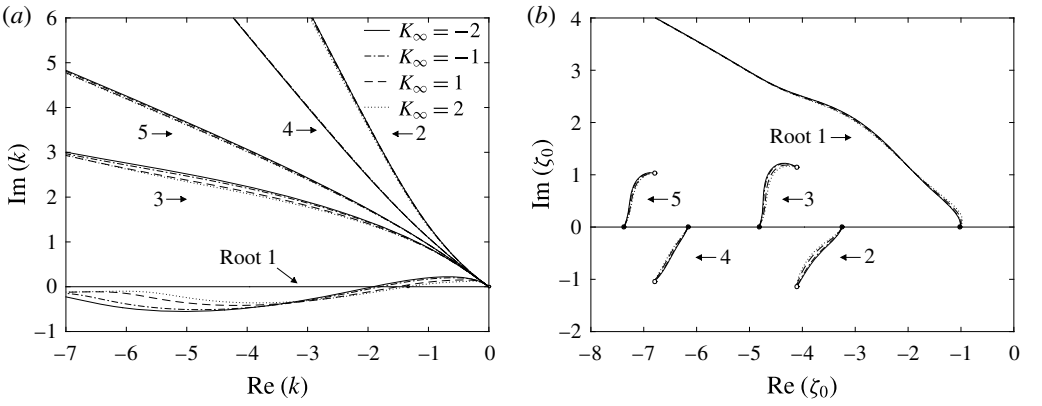

FIGURE 3. The first five roots of the dispersion equation in the (*a*) k-plane and (*b*) ζ_0-plane.

The above equation has an infinite number of roots, all of them lying on the negative real semi-axis in the ζ_0-plane. This suggests that the dispersion equation (5.44) has an infinite number of roots. In figure 3 we show five of these. Each root was calculated by using the corresponding root of (5.45) as an initial guess for a small value of ω. Then the dispersion relation (5.44) was solved using Newton iterations, where the frequency was kept fixed until the iteration process converged and the corresponding value of ζ_0 was found. The process was then repeated for a new, larger value of ω. The results of the calculations are shown in figure 3. We see that in the ζ_0-plane, all the roots originate from the points defined by (5.45), and all of them, except the first one, tend to finite points in the ζ_0-plane as $\omega \to \infty$. In this limit the dispersion equation (5.44) reduces to

$$\int_{\zeta_0}^{\infty} \mathrm{Ai}(s)\,\mathrm{d}s = 0. \tag{5.46}$$

Equation (5.46) has an infinite number of roots, which all come in complex conjugate pairs and lie in the left half of the ζ_0-plane. As far as the first root is concerned, its behaviour is different. For this root, ζ_0 moves to infinity as $\omega \to \infty$ (see figure 3*b*). This root also behaves differently in the k-plane. While all the other roots remain in the second quadrant for all ω, representing the modes that decay downstream, the first root crosses the real axis at point $k = k_0 < 0$ at a critical value ω_0 of the frequency ω. Both k_0 and ω_0 depend on the Kármán–Guderley parameter. This root represents the Tollmien–Schlichting wave, which appears to be neutral at $\omega = \omega_0$. For all $\omega > \omega_0$ this root remains in the third quadrant, which signifies that the Tollmien–Schlichting wave is growing downstream. It is interesting to note that $|k_0|$ decreases as the Kármán–Guderley parameter K_∞ increases (see Ryzhov 2012).

A way to determine how k_0 depends on K_∞ was suggested by Timoshin (1990). He noticed that, in the case of neutral perturbations, the transonic dispersion equation (5.44) can easily be reduced to the dispersion equation for incompressible flow:

$$(\mathrm{i}k)^{1/3}|k|[\mathrm{Ai}'(\zeta_0)]^{-1} \int_{\zeta_0}^{\infty} \mathrm{Ai}(s)\,\mathrm{d}s = 1. \tag{5.47}$$

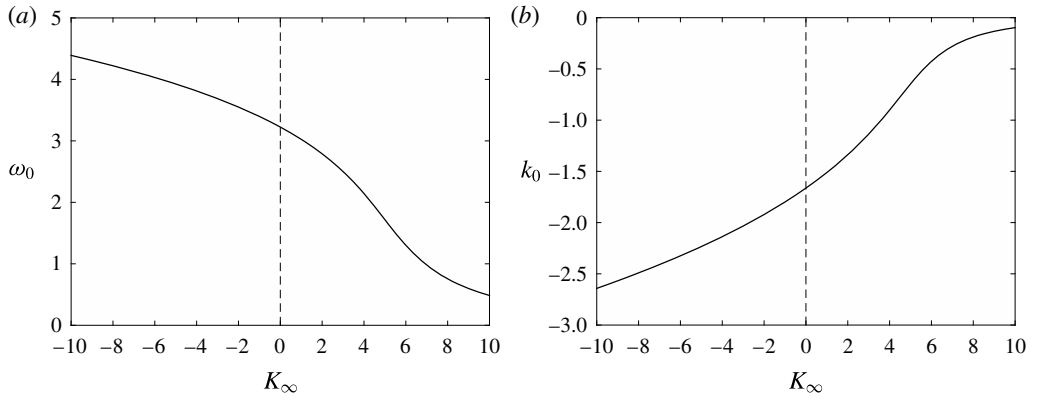

FIGURE 4. (*a*) Neutral frequency and (*b*) wavenumber as functions of the Kármán–Guderley parameter.

To perform this task, it is convenient to introduce the phase velocity $c_0 = \omega_0/k_0$, and perform the affine transformations

$$c_0 = ac_0^*, \quad k_0 = a^{-3}k_0^*, \tag{5.48a,b}$$

where $c_0^* = -2.296$, $k_0^* = -1.00049$ is the neutral solution of (5.47). The transformations (5.48) turn (5.44) into

$$(\mathrm{i}k_0^*)^{1/3}|k_0^*|[\mathrm{Ai}'(\zeta_0^*)]^{-1}\int_{\zeta_0^*}^{\infty}\mathrm{Ai}(s)\,\mathrm{d}s = a^4(-2ac_0^* - K_\infty)^{1/2}, \tag{5.49}$$

Comparison of (5.47) with (5.49) leads to the following equation for constant a:

$$a^8(2ac_0^* + K_\infty) = -1. \tag{5.50}$$

This equation has only one real solution whose behaviour is shown in figure 4.

Let us now return to the integral (5.43). Our intention is to deform the integration path in the k-plane. We shall distinguish between two cases: subsonic ($K_\infty < 0$) and supersonic ($K_\infty > 0$). In both cases we start by considering a value of the frequency that is smaller than the critical frequency. For such ω, all the roots of (5.44) lie in the second quadrant of the complex k-plane. We have to remember that, when introducing an analytical branch of the function $(\mathrm{i}k)^{1/3}$, we had to make a branch cut along the positive imaginary axis in the k-plane. Therefore, we have to split the integration interval in (5.43) into two parts, negative and positive real semi-axes.

In the case of negative K_∞, we close the contour along the real negative semi-axis with an arc C_S^- of a large radius R and a ray C_I^- originating at the coordinate origin (see figure 5*a*). The angle between the negative real semi-axis and C_I^- is chosen so that the closed contour encloses only one root k_1. To calculate the integral along the real positive semi-axis, we introduce two closed contours ($C_{R_2}^+$, $C_{E_2}^+$, $C_{S_2}^+$, C_I^+) and ($C_{R_3}^+$, $C_{S_3}^+$, $C_{E_3}^+$) divided by the point $k = 2\omega/|K_\infty|$ on the real axis.

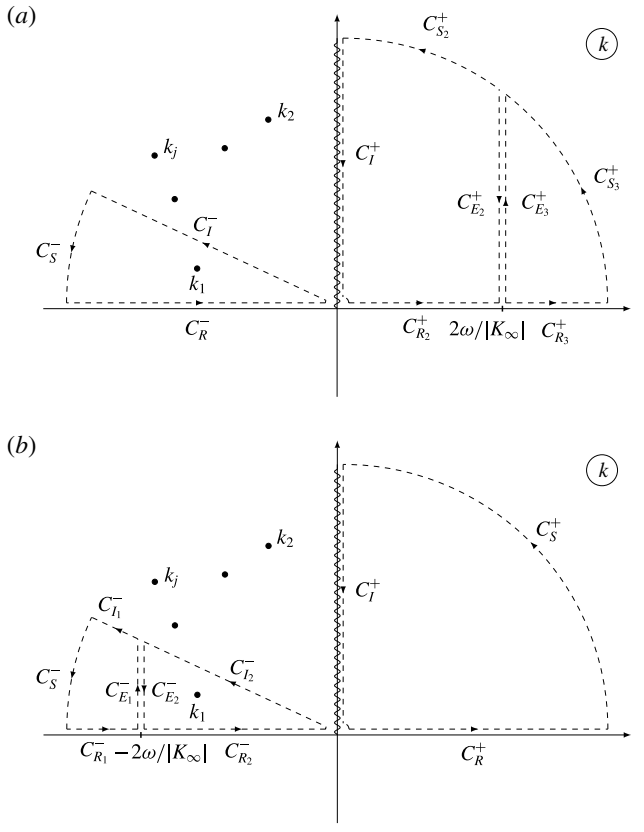

FIGURE 5. The contour of integration in the k-plane for (a) negative and (b) positive values of the Kármán–Guderley parameter.

Using the residue theorem and setting $R \to \infty$, we can then write (5.43) as

$$P(t,x) = -\frac{3\mathrm{i}q_1k_1^2\mathrm{Ai}'(\zeta_0)\displaystyle\int_{\zeta_0}^{\infty}\varphi(s)\,\mathrm{d}s\,\bar{F}(k_1)\mathrm{e}^{\mathrm{i}(\omega t+k_1x)}}{3\mathrm{Ai}'(\zeta_0)[K_\infty k_1+\omega]+q_1(\mathrm{i}k_1)^{1/3}\left[2\mathrm{Ai}(\zeta_0)\zeta_0\left(q_1\dfrac{\omega}{k_1^2}+k_1\right)+7k_1I_{\zeta_0}\right]} - \frac{\mathrm{e}^{\mathrm{i}\omega t}}{2\pi}\left[\int_{C_I^-}+\int_{C_I^+}\right], \tag{5.51}$$

where

$$q_1=\sqrt{-K_\infty k_1^2-2\omega k_1}, \quad I_{\zeta_0}=\int_{\zeta_0}^{\infty}\mathrm{Ai}(s)\,\mathrm{d}s, \quad \zeta_0=\frac{\mathrm{i}\omega}{(\mathrm{i}k_1)^{2/3}}. \tag{5.52a–c}$$

The first term in the above equation is the residue at point k_1. Note that, using the Jordan lemma, we have disregarded the integrals along C_S^-, $C_{S_2}^+$ and $C_{S_3}^+$. Further, using the Watson lemma, it may be shown (see Bernots 2014) that at large values of x the

contribution of the integrals along the rays C_I^- and C_I^+ in (5.51) amounts to

$$-\frac{(\mathrm{i}+1)\Gamma(\frac{29}{6})\bar{F}(0)}{24\pi\omega^{5/2}\mathrm{Ai}'(0)|K_\infty|^{1/2}}\frac{\mathrm{e}^{\mathrm{i}\omega t}}{x^{29/6}}+\cdots. \tag{5.53}$$

Thus we can conclude that at large values of x and negative values of the Kármán–Guderley parameter,

$$P(t,x)=\mathscr{K}(\omega,K_\infty)\bar{F}(k_1)\mathrm{e}^{\mathrm{i}(\omega t+k_1 x)}-\frac{(\mathrm{i}+1)\Gamma(\frac{29}{6})\bar{F}(0)}{24\pi\omega^{5/2}\mathrm{Ai}'(0)|K_\infty|^{1/2}}\frac{\mathrm{e}^{\mathrm{i}\omega t}}{x^{29/6}}+\cdots, \tag{5.54}$$

where $\mathscr{K}(\omega,K_\infty)$ is the receptivity coefficient. It is a function of the frequency ω and the Kármán–Guderley parameter K_∞. It is calculated as

$$\mathscr{K}=-\frac{3\mathrm{i}q_1k_1^2\mathrm{Ai}'(\zeta_0)\displaystyle\int_{\zeta_0}^{\infty}\varphi(s)\,\mathrm{d}s}{3\mathrm{Ai}'(\zeta_0)[K_\infty k_1+\omega]+q_1(\mathrm{i}k_1)^{1/3}\left[2\mathrm{Ai}(\zeta_0)\zeta_0\left(q_1\dfrac{\omega}{k_1^2}+k_1\right)+7k_1I_{\zeta_0}\right]}. \tag{5.55}$$

The above analysis can be repeated for positive K_∞, now deforming the contour of integration as shown in figure 5(*b*). Interestingly, the results of the analysis can be expressed again by (5.54) and (5.55). The first term on the right-hand side of (5.54) represents the Tollmien–Schlichting wave. Its amplitude is given by the product of the receptivity coefficient $\mathscr{K}$ and the Fourier transform of the roughness shape function $\bar{F}(k_1)$ calculated at $k=k_1$.

The results of the numerical calculation of the receptivity coefficient are shown in figures 6 and 7. It is interesting to note that $|\mathscr{K}|$ reaches its maximum when $K_\infty=0$, i.e. the free-stream Mach number M_∞ is exactly one.

6. Nonlinear receptivity problem

We shall now assume that the roughness height parameter h is an order-one quantity. The amplitude α of the acoustic wave will still be assumed small. In this case the solution of the viscous–inviscid interaction problem (4.21)–(4.25) can be represented in the form

$$\left.\begin{aligned} u(x,y,t)&=u_0(x,y)+\alpha u_1(x,y,t)+\cdots,\\ v(x,y,t)&=v_0(x,y)+\alpha v_1(x,y,t)+\cdots,\\ p(x,t)&=p_0(x)+\alpha p_1(x,t)+\cdots,\\ A(x,t)&=A_0(x)+\alpha A_1(x,t)+\cdots,\\ P(x,Y,t)&=P_0(x,Y)+\alpha P_1(x,Y,t)+\cdots. \end{aligned}\right\} \tag{6.1}$$

6.1. *Nonlinear steady solution*

Setting $\alpha=0$ in (4.21) and (4.22) gives the equations for the steady flow past the roughness in the lower deck:

$$u_0\frac{\partial u_0}{\partial x}+v_0\frac{\partial u_0}{\partial y}=-\frac{\partial p_0}{\partial x}+\frac{\partial^2 u_0}{\partial y^2}, \tag{6.2a}$$

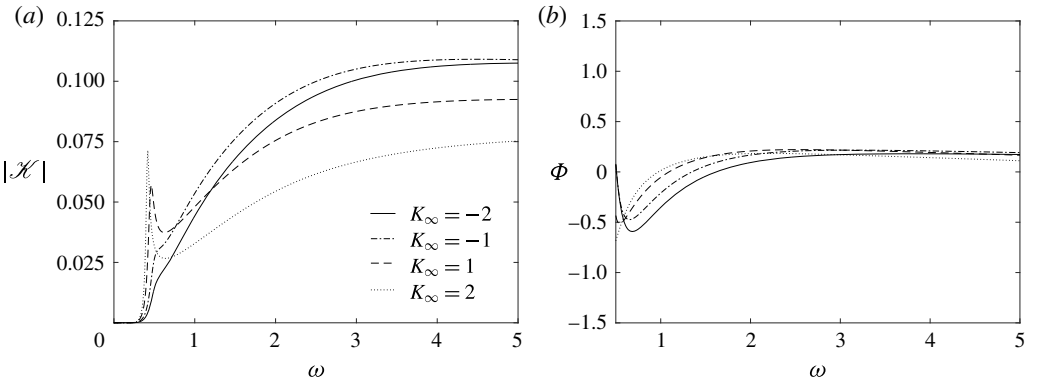

FIGURE 6. Receptivity coefficient modulus (*a*) and argument (*b*).

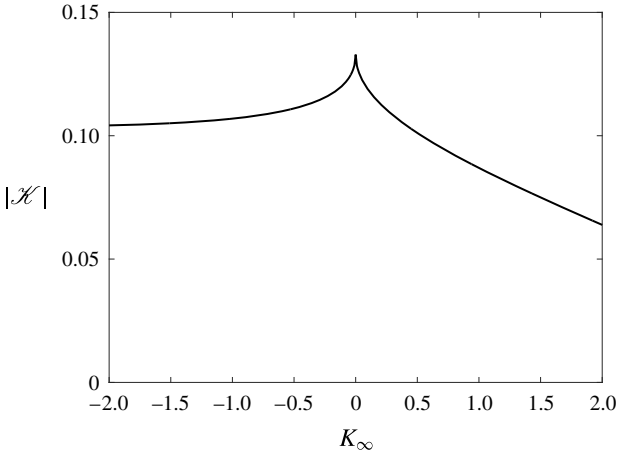

FIGURE 7. Dependence of the receptivity coefficient on K_∞ for neutral ω_0 and k_0.

$$\frac{\partial u_0}{\partial x} + \frac{\partial v_0}{\partial y} = 0. \tag{6.2b}$$

These have to be solved with the following boundary conditions:

$$u_0 = v_0 = 0 \quad \text{at } y = 0, \tag{6.3a}$$

$$u_0 = y + \cdots \quad \text{as } x \to -\infty, \tag{6.3b}$$

$$u_0 = y + A_0(x) + \cdots \quad \text{as } y \to \infty. \tag{6.3c}$$

The pressure p_0 in (6.2*a*) is not known in advance, and has to be found using the transonic small perturbation equation (4.23). For a steady flow it assumes the form

$$K_\infty \frac{\partial^2 P_0}{\partial x^2} - \frac{\partial^2 P_0}{\partial Y^2} = 0. \tag{6.4}$$

Substitution of (6.1) and (5.1) into boundary condition (4.24*a*) renders it in the form

$$\frac{\partial P_0}{\partial Y} = \frac{\mathrm{d}^2 A_0}{\mathrm{d}x^2} - h\frac{\mathrm{d}^2 F}{\mathrm{d}x^2} \quad \text{at } Y = 0. \tag{6.5}$$

If the flow is supersonic ($K_\infty > 0$), then the general solution to (6.4) is written as

$$P_0 = f_1(x - \sqrt{K_\infty}Y) + f_2(x + \sqrt{K_\infty}Y), \tag{6.6}$$

with the two terms representing the perturbations that propagate downstream and upstream, respectively. The causality rule suggests that the second term should be disregarded. Taking this into account, and using boundary condition (6.5), one can find that at the 'bottom' of the upper deck the Ackeret formula holds:

$$P_0(x) = \frac{hF'(x) - A_0'(x)}{\sqrt{K_\infty}}, \quad K_\infty > 0. \tag{6.7}$$

In subsonic flow ($K_\infty < 0$) the solution of (6.4) satisfying boundary condition (6.5) and the condition of attenuation of the perturbations as $Y \to \infty$ is expressed by the Hilbert integral of thin airfoil theory:

$$P_0(x) = \frac{1}{\pi\sqrt{-K_\infty}} \int_{-\infty}^{\infty} \frac{hF'(s) - A_0'(s)}{s - x}\,\mathrm{d}s, \quad K_\infty < 0. \tag{6.8}$$

To solve the steady viscous–inviscid interaction problem as formulated above, we used the numerical technique suggested by Kravtsova, Zametaev & Ruban (2005). We shall give here a short description of the method. For more details, the reader is referred to the original paper of Kravtsova *et al.* (2005). To perform the calculations, we introduce a discrete mesh $\{x_i\}$, where $i = 1, \ldots, N$, and denote the vector composed of the values of A_0 at the mesh points by $\boldsymbol{A}$. We also consider the vector $\boldsymbol{B}$ whose elements are the values of the pressure gradient $\mathrm{d}p/\mathrm{d}x$ at the mesh points. Then, the finite-difference representation of the inviscid equations (6.7) and (6.8) can be expressed in the form

$$\boldsymbol{B}|_{inv} = \boldsymbol{L}(\boldsymbol{A}), \tag{6.9}$$

where $\boldsymbol{L}$ is a linear operator. Also, given the displacement function $\boldsymbol{A}$, equations (6.2) and (6.3) allow us to calculate the velocity field (u_0, v_0) in the viscous sublayer and the pressure gradient. The latter may be expressed in the form

$$\boldsymbol{B}|_{vis} = \boldsymbol{N}(\boldsymbol{A}), \tag{6.10}$$

where $\boldsymbol{N}$ is a nonlinear operator. Our task is to find $\boldsymbol{A}$ such that the pressure gradient (6.9) defined by the outer solution coincides with the pressure gradient (6.10) defined by the inner solution. Following the formalism of the Newtonian method, we start with an approximate distribution of the displacement function $\widetilde{\boldsymbol{A}}$ and introduce a correction, $\delta\boldsymbol{A}$. Then, assuming $\delta\boldsymbol{A}$ to be small, equations (6.9) and (6.10) may be written as

$$\boldsymbol{B}|_{inv} = \boldsymbol{L}(\widetilde{\boldsymbol{A}}) + \frac{\partial \boldsymbol{L}}{\partial \boldsymbol{A}}\delta\boldsymbol{A}, \quad \boldsymbol{B}|_{vis} = \boldsymbol{N}(\widetilde{\boldsymbol{A}}) + \frac{\partial \boldsymbol{N}}{\partial \boldsymbol{A}}\,\delta\boldsymbol{A}. \tag{6.11a,b}$$

The requirement that the pressure gradient should be the same in the viscous sublayer and at the 'bottom' of the upper deck leads to the following equation for the correction $\delta\boldsymbol{A}$:

$$\left(\frac{\partial \boldsymbol{L}}{\partial \boldsymbol{A}} - \frac{\partial \boldsymbol{N}}{\partial \boldsymbol{A}}\right)\delta\boldsymbol{A} = \boldsymbol{N}(\widetilde{\boldsymbol{A}}) - \boldsymbol{L}(\widetilde{\boldsymbol{A}}). \tag{6.12}$$

The most time-consuming part of the numerical procedure is the calculation of the elements of the matrices $\boldsymbol{L}$ and $\boldsymbol{N}$. On each iteration, we first calculate the 'viscous'

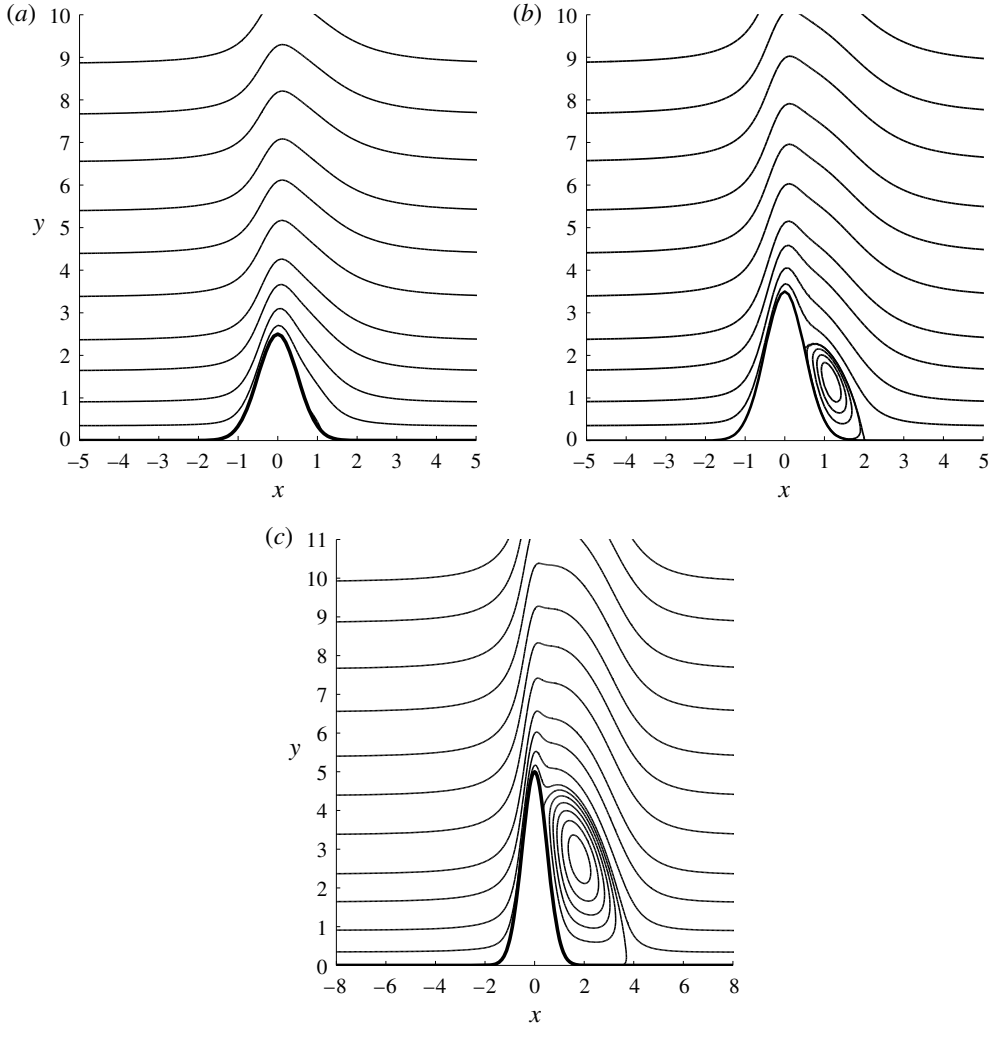

FIGURE 8. Streamlines for the steady flow, $K_\infty = -2$: (*a*) $h = 2.5$; (*b*) $h = 3.5$; (*c*) $h = 5.0$.

and 'inviscid' pressure gradients for a given $\widetilde{\boldsymbol{A}}$, and then repeat the calculations N times with the displacement function perturbed at a single point x_i. Comparing the perturbed and unperturbed results allows us to determine the ith columns in matrices $\boldsymbol{L}$ and $\boldsymbol{N}$.

Some of the results of the calculations are shown in figure 8 in the form of streamline patterns. Here we choose the Kármán–Guderley parameter to be $K_\infty = -2$, and the shape of the roughness $F = \mathrm{e}^{-2x^2}$. In this case the separation region forms when the roughness height is $h = 2.5$, and it increases in size as h is growing.

6.2. *Unsteady problem formulation*

The equations for the unsteady perturbations are obtained by substituting (6.1) into (4.21) and (4.22), and working with $O(\alpha)$ terms. We find that in the viscous sublayer

the flow is described by the linear boundary-layer equations

$$\frac{\partial u_1}{\partial t}+u_0\frac{\partial u_1}{\partial x}+u_1\frac{\partial u_0}{\partial x}+v_0\frac{\partial u_1}{\partial y}+v_1\frac{\partial u_0}{\partial y}=\cos(\omega t)-\frac{\partial p_1}{\partial x}+\frac{\partial^2 u_1}{\partial y^2}, \tag{6.13a}$$

$$\frac{\partial u_1}{\partial x}+\frac{\partial v_1}{\partial y}=0. \tag{6.13b}$$

These have to be solved with the no-slip conditions of the surface of the roughness,

$$u_1=v_1=0, \quad y=0, \tag{6.13c}$$

the condition of matching with the solution in the middle deck,

$$u_1=A_1(x,t)+\frac{1}{\omega}\sin(\omega t)+\cdots, \quad y\to+\infty, \tag{6.13d}$$

and the condition of matching with the solution upstream of the roughness,

$$u_1=\frac{1}{\omega}\left\{\left[1-\mathrm{e}^{-\sqrt{\omega/2}y}\cos\left(\sqrt{\frac{\omega}{2}}y\right)\right]\sin(\omega t)+\mathrm{e}^{-\sqrt{\omega/2}y}\sin\left(\sqrt{\frac{\omega}{2}}y\right)\cos(\omega t)\right\}+\cdots \quad \text{as } x\to-\infty. \tag{6.13e}$$

In the upper tier we have to solve (5.18) subject to the boundary conditions (5.19). In the notation used here, these are written as

$$K_\infty\frac{\partial^2 P_1}{\partial x^2}+2\frac{\partial^2 P_1}{\partial x\partial t}=\frac{\partial^2 P_1}{\partial Y^2}, \tag{6.14a}$$

$$\frac{\partial P_1}{\partial Y}=\frac{\partial^2 A_1}{\partial x^2} \quad \text{at } Y=0, \tag{6.14b}$$

$$P_1=0 \quad \text{as } Y\to\infty. \tag{6.14c}$$

We shall seek the solution in the viscous sublayer in the form

$$\left.\begin{aligned} u_1&=u_{11}\sin(\omega t)+u_{12}\cos(\omega t),\\ v_1&=v_{11}\sin(\omega t)+v_{12}\cos(\omega t),\\ p_1&=p_{11}\sin(\omega t)+p_{12}\cos(\omega t),\\ A_1&=A_{11}\sin(\omega t)+A_{12}\cos(\omega t).\end{aligned}\right\} \tag{6.15a–d}$$

Substitution of (6.15) into (6.13) results in the following set of linear equations:

$$-\omega u_{12}+u_0\frac{\partial u_{11}}{\partial x}+u_{11}\frac{\partial u_0}{\partial x}+v_0\frac{\partial u_{11}}{\partial y}+v_{11}\frac{\partial u_0}{\partial y}=-\frac{\partial p_{11}}{\partial x}+\frac{\partial^2 u_{11}}{\partial y^2}, \tag{6.16a}$$

$$\omega u_{11}+u_0\frac{\partial u_{12}}{\partial x}+u_{12}\frac{\partial u_0}{\partial x}+v_0\frac{\partial u_{12}}{\partial y}+v_{12}\frac{\partial u_0}{\partial y}=1-\frac{\partial p_{12}}{\partial x}+\frac{\partial^2 u_{12}}{\partial y^2}, \tag{6.16b}$$

$$\frac{\partial u_{11}}{\partial x}+\frac{\partial v_{11}}{\partial y}=0, \quad \frac{\partial u_{12}}{\partial x}+\frac{\partial v_{12}}{\partial y}=0. \tag{6.16c,d}$$

These have to be solved subject to the boundary conditions

$$u_{11} = u_{12} = v_{11} = v_{12} = 0, \quad y = 0, \tag{6.17a}$$

$$u_{11} = A_{11}(x) + \frac{1}{\omega} + \cdots, \quad u_{12} = A_{12}(x) + \cdots, \quad y \to +\infty, \tag{6.17b,c}$$

$$u_{11} = \frac{1}{\omega}\left[1 - \exp\left(-\sqrt{\frac{\omega}{2}}y\right)\cos\left(\sqrt{\frac{\omega}{2}}y\right)\right], \tag{6.17d}$$

$$u_{12} = \frac{1}{\omega}\exp\left(-\sqrt{\frac{\omega}{2}}y\right)\sin\left(\sqrt{\frac{\omega}{2}}y\right), \quad x \to -\infty. \tag{6.17e}$$

6.3. *Transonic interaction law for* $K_\infty < 0$

Now our task will be to express the solution of (6.14*a*) for the upper deck in a form suitable for numerical analysis. We assume that the solution is periodic in time, namely,

$$P_1 = \mathrm{e}^{\mathrm{i}\omega t}\widetilde{P} + \text{c.c.} \tag{6.18}$$

Substitution of (6.18) into (6.14*a*) yields

$$K_\infty \frac{\partial^2 \widetilde{P}}{\partial x^2} + 2\mathrm{i}\omega \frac{\partial \widetilde{P}}{\partial x} = \frac{\partial^2 \widetilde{P}}{\partial Y^2}. \tag{6.19}$$

The above equation can be reduced to the Helmholtz equation

$$\nabla^2 p_v + \frac{\omega^2}{K_\infty^2} p_v = 0 \tag{6.20}$$

by means of the transformations

$$\widetilde{P} = \mathrm{e}^{-\mathrm{i}(\omega/K_\infty)x} p_v(x, y_1), \quad y_1 = \sqrt{-K_\infty}\, Y. \tag{6.21}$$

Similar to the pressure P_1, we represent the displacement function A_1 in the time-periodic form

$$A_1 = \mathrm{e}^{\mathrm{i}\omega t}\widetilde{A} + \text{c.c.}, \tag{6.22}$$

and then the boundary condition (6.14*b*) turns into

$$\left.\frac{\partial p_v}{\partial y_1}\right|_{y_1=0} = g_1(x), \tag{6.23}$$

where

$$g_1(x) = \frac{1}{\sqrt{-K_\infty}}\mathrm{e}^{\mathrm{i}(\omega/K_\infty)x}\widetilde{A}''(x). \tag{6.24}$$

Let us introduce a point source in (6.20) centred at point (x_0, y_{10}):

$$\nabla^2 V + \frac{\omega^2}{K_\infty^2} V = \delta(x - x_0, y_1 - y_{10}), \tag{6.25}$$

where δ is the Dirac delta function. The two fundamental solutions of (6.25), which are functions of the distance $r = \sqrt{(x - x_0)^2 + (y_1 - y_{10})^2}$ from the source only, are

$$V_1 = -\frac{\mathrm{i}}{4}\mathrm{H}_0^{(1)}\left(\frac{\omega}{-K_\infty}r\right), \quad V_2 = \frac{\mathrm{i}}{4}\mathrm{H}_0^{(2)}\left(\frac{\omega}{-K_\infty}r\right), \tag{6.26a,b}$$

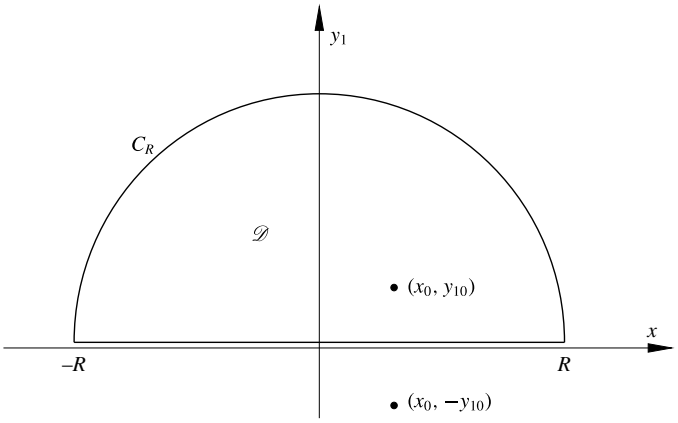

FIGURE 9. Region $\mathscr{D}$ used in equation (6.29).

where $\mathrm{H}_0^{(1)}$ and $\mathrm{H}_0^{(2)}$ are Hankel functions. It is well known that (see e.g. Abramowitz & Stegun 1965)

$$\left.\begin{aligned} \mathrm{H}_0^{(1)}(z) &= \sqrt{\frac{2}{\pi z}}\,\mathrm{e}^{\mathrm{i}(z-\pi/4)} + \cdots, \\ \mathrm{H}_0^{(2)}(z) &= \sqrt{\frac{2}{\pi z}}\,\mathrm{e}^{-\mathrm{i}(z-\pi/4)} + \cdots \end{aligned}\right\} \quad \text{as } z \to \infty. \tag{6.27}$$

Substituting (6.27) into (6.26) and using $V_{1,2}$ instead of p_v in (6.21), we find from (6.18) that, at large values of y_1,

$$P_1^{(1)} = -\mathrm{i}\sqrt{\frac{-K_\infty}{\pi\omega y_1}}\,\exp\left\{\mathrm{i}\left[\omega t + \frac{\omega}{(-K_\infty)}y_1 + \frac{\omega}{(-K_\infty)}x - \frac{\pi}{4}\right]\right\} + \cdots, \tag{6.28a}$$

$$P_1^{(2)} = \mathrm{i}\sqrt{\frac{-K_\infty}{\pi\omega y_1}}\,\exp\left\{\mathrm{i}\left[\omega t - \frac{\omega}{(-K_\infty)}y_1 + \frac{\omega}{(-K_\infty)}x + \frac{\pi}{4}\right]\right\} + \cdots. \tag{6.28b}$$

We see that (6.28*a*,*b*) represent the perturbations propagating in the negative and positive y_1-direction, respectively. Since we are interested in the perturbations radiated by the roughness, we will be using the second of the solutions (6.26).

Let us consider region $\mathscr{D}$ inside a closed contour that is composed of a semicircle C_R of a large radius R and a segment $[-R, R]$ of the x-axis (see figure 9). Green's formula applied to this region is written as

$$\begin{aligned} \iint_{\mathscr{D}} (U\nabla^2 V - V\nabla^2 U)\,\mathrm{d}x\,\mathrm{d}y_1 \;=\; & \int_{-R}^{R} \left(U\frac{\partial V}{\partial n} - V\frac{\partial U}{\partial n}\right)\bigg|_{y_1=0} \mathrm{d}x \\ & + \int_{C_R} \left(U\frac{\partial V}{\partial n} - V\frac{\partial U}{\partial n}\right) \mathrm{d}s, \end{aligned} \tag{6.29}$$

We choose U in (6.29) to coincide with p_v, and V to coincide with the second function in (6.26). Keeping in mind that $V \sim 1/\sqrt{y_1}$ and p_v has to satisfy the attenuation condition, we can disregard the second integral on the right-hand side of (6.29). It follows from (6.20) and (6.25) that, in region $\mathscr{D}$,

$$U\nabla^2 V - V\nabla^2 U = p_v(x, y_1)\delta(x - x_0, y_1 - y_{10}). \tag{6.30}$$

Using (6.30) in the integral on the left-hand side of (6.29), we have

$$p_v(x_0, y_{10}) = \int_{-\infty}^{\infty} \left(U\frac{\partial V}{\partial n} - V\frac{\partial U}{\partial n} \right)\Big|_{y_1=0} \mathrm{d}x. \tag{6.31}$$

Keeping in mind that n is the external normal to region $\mathscr{D}$, and using the boundary condition (6.23) for U, we have

$$\left(U\frac{\partial V}{\partial n} - V\frac{\partial U}{\partial n} \right)\Big|_{y_1=0} = V_2 g_1(x) - p_v\frac{\partial V_2}{\partial y_1}, \tag{6.32}$$

which turns (6.31) into

$$p_v(x_0, y_{10}) = \int_{-\infty}^{\infty} \left(V_2^{(+)} g_1(x) - p_v\frac{\partial V_2^{(+)}}{\partial y_1} \right)\Big|_{y_1=0} \mathrm{d}x. \tag{6.33}$$

Here the superscript $(+)$ in $V_2^{(+)}$ is used to indicate that $V_2^{(+)}$ is the solution of (6.25) with the source situated at point (x_0, y_0) above the x-axis.

Let us now reflect the source in the x-axis (see figure 9), and write (6.25) in the form

$$\nabla^2 V + \frac{\omega^2}{K_\infty^2} V = \delta(x - x_0, y_1 + y_{10}). \tag{6.34}$$

Our interest again is in the second of the solutions (6.26), which describes the perturbations radiated by the roughness. We shall write it as

$$V_2^{(-)} = \frac{\mathrm{i}}{4} H_0^{(2)}\left(\frac{\omega}{-K_\infty} r \right), \tag{6.35}$$

where $r = \sqrt{(x - x_0)^2 + (y_1 + y_{10})^2}$. If we choose $U = p_v$ and $V = V_2^{(-)}$ in Green's formula (6.29), and take into account that now the source is situated outside region $\mathscr{D}$, then instead of (6.33) we will have

$$\int_{-\infty}^{\infty} \left(V_2^{(-)} g_1(x) - p_v\frac{\partial V_2^{(-)}}{\partial y_1} \right)\Big|_{y_1=0} \mathrm{d}x = 0. \tag{6.36}$$

It is easily seen that

$$V_2^{(+)}|_{y_1=0} = V_2^{(-)}|_{y_1=0}, \qquad \frac{\partial V_2^{(+)}}{\partial y_1}\bigg|_{y_1=0} = -\frac{\partial V_2^{(-)}}{\partial y_1}\bigg|_{y_1=0}, \tag{6.37a,b}$$

which means that p_v can be eliminated from the integral on the right-hand side of (6.33) by simply adding (6.36) to (6.33). This results in

$$p_v(x_0, y_{10}) = 2\int_{-\infty}^{\infty} g_1(x) V_2^{(+)}\Big|_{y_1=0} \,\mathrm{d}x. \tag{6.38}$$

Making use of (6.24) and of the second of the solutions (6.26), we can write (6.38) in the form

$$p_v(x, y_1) = \frac{\mathrm{i}}{2\sqrt{-K_\infty}} \int_{-\infty}^{\infty} \mathrm{e}^{\mathrm{i}(\omega/K_\infty)\xi} H_0^{(2)}\left(\frac{\omega}{-K_\infty}\sqrt{(x-\xi)^2 + y_1^2}\right) \widetilde{A}''(\xi)\,\mathrm{d}\xi. \tag{6.39}$$

It remains to return to (6.21), and we can conclude that the solution in the upper deck is written as

$$\widetilde{P} = \frac{\mathrm{i}}{2\sqrt{-K_\infty}} \int_{-\infty}^{\infty} \mathrm{e}^{\mathrm{i}(\omega/K_\infty)(\xi-x)} H_0^{(2)}\left(\frac{\omega}{-K_\infty}\sqrt{(x-\xi)^2 - K_\infty Y^2}\right) \widetilde{A}''(\xi)\,\mathrm{d}\xi. \tag{6.40}$$

When performing the unsteady flow calculations, we used the above equation to form the matrix $\boldsymbol{L}$ in (6.9). The rest of the numerical procedure is the same as in § 6.1. The results of the calculations are presented in figures 10 and 11. In figure 10 we show the pressure gradient distribution along the body surface for a particular value of the Kármán–Guderley parameter $K_\infty = -1$. According to the linear theory (see § 5), the neutral frequency for $K_\infty = -1$ is $\omega_0 = 3.35$ (see figure 4*a*). Figure 10 shows that the perturbations decay downstream of the roughness if $\omega < \omega_0$, and start growing if $\omega > \omega_0$.

Figure 11 shows how the receptivity coefficient $\mathscr{K}$ depends on the roughness height h. Here, for each value of the Kármán–Guderley parameter, we chose the frequency ω to coincide with the neutral frequency (see figure 4*a*), and repeated the calculations for a sequence of values of h. We then determined the amplitude of the oscillations of the pressure gradient in the Tollmien–Schlichting wave downstream of the roughness. The receptivity coefficient is the ratio of this amplitude and the roughness height h. It is interesting to note that the receptivity coefficient starts to grow rapidly as soon as the separation region forms in the flow past the roughness (see figure 8).

6.4. *Transonic interaction law for* $K_\infty > 0$

For positive values of the Kármán–Guderley parameter, we treat the upper-deck equation (6.14*a*) in a slightly different way. We start as before by representing the solution in the time-periodic form (6.18) and use the transformation (6.21), this time without scaling of the independent variable Y. This results in the 'telegraph equation':

$$\frac{\partial^2 p_v}{\partial Y^2} = K_\infty \frac{\partial^2 p_v}{\partial x^2} + \frac{\omega^2}{K_\infty} p_v. \tag{6.41}$$

This has to be solved with the boundary condition

$$\left.\frac{\partial p_v}{\partial Y}\right|_{Y=0} = g_2(x), \tag{6.42}$$

where

$$g_2(x) = \mathrm{e}^{\mathrm{i}(\omega/K_\infty)x}\widetilde{A}''(x). \tag{6.43}$$

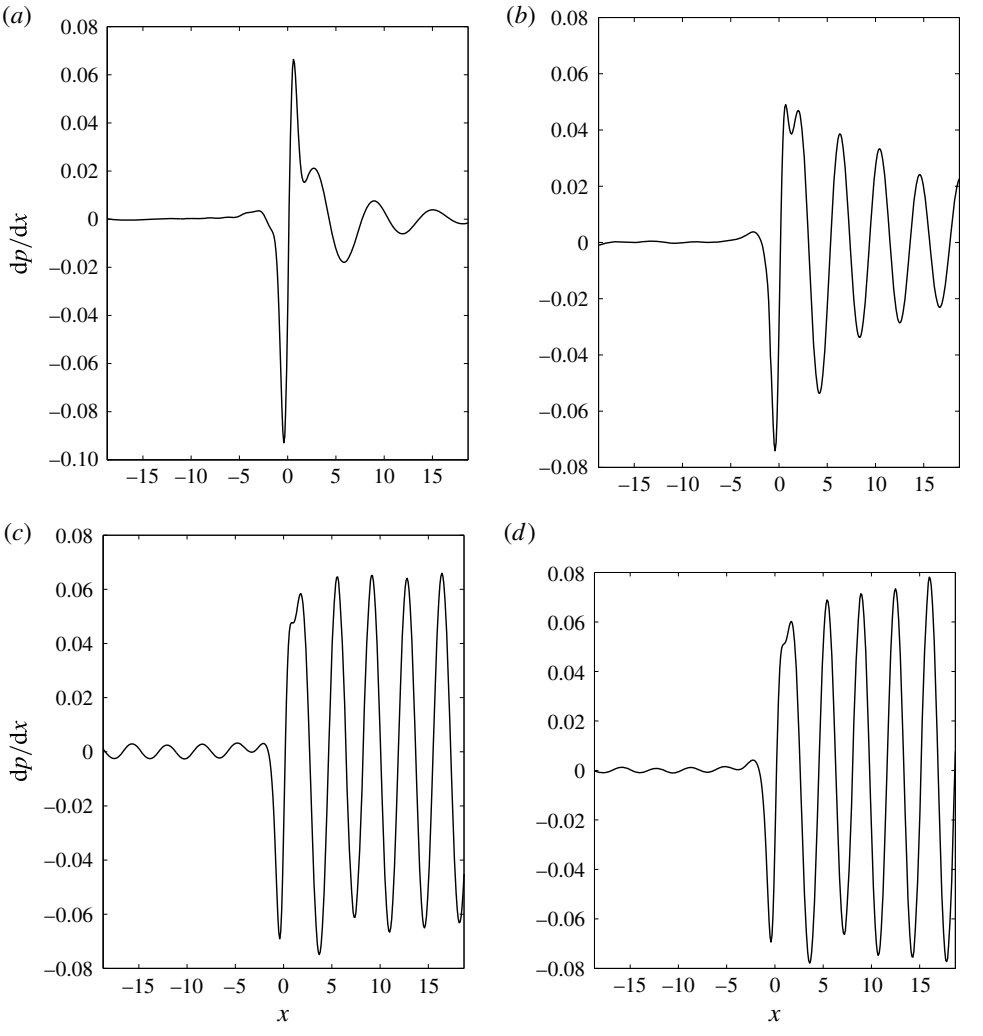

FIGURE 10. Pressure gradient distribution for $h=0.2$ and $K_\infty=-1$: (*a*) $\omega=1.7$; (*b*) $\omega=2.8$; (*c*) $\omega=3.35$; (*d*) $\omega=3.45$.

A fundamental solution of (6.41) may be sought in the form

$$p_v(x, Y)=f(\eta), \quad \eta=\frac{\omega}{K_\infty}\sqrt{x^2-K_\infty Y^2}. \tag{6.44a,b}$$

Substitution of (6.44) into (6.41) leads to the Bessel equation

$$f''+\frac{1}{\eta}f'+f=0. \tag{6.45}$$

This means that the solution of (6.41) may be written as

$$p_v(x, Y)=\int_{-\infty}^{x-\sqrt{K_\infty}Y}\varphi(\xi)\mathrm{J}_0\left(\frac{\omega}{K_\infty}\sqrt{(x-\xi)^2-K_\infty Y^2}\right)\mathrm{d}\xi, \tag{6.46}$$

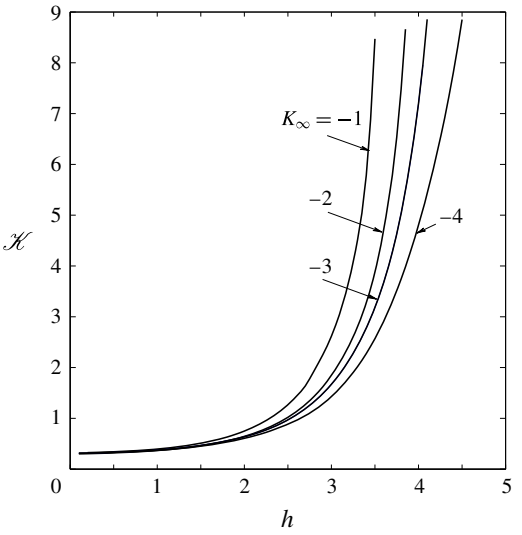

FIGURE 11. The receptivity coefficients $\mathscr{K}$ for negative values of the Kármán–Guderley parameter K_∞.

where J_0 is the Bessel function. To find the function $\varphi(\xi)$, one has to use the boundary condition (6.42). Differentiation of (6.46) with respect to Y yields

$$\frac{\partial p_v}{\partial Y} = -\sqrt{K_\infty}\varphi(x - \sqrt{K_\infty}Y) - \int_{-\infty}^{x-\sqrt{K_\infty}Y} \frac{\omega Y \mathrm{J}_0'}{\sqrt{(x-\xi)^2 - K_\infty Y^2}}\,\mathrm{d}\xi. \tag{6.47}$$

Setting $Y = 0$ in (6.47) and using (6.42) and (6.43) it is easily found that

$$\varphi(x) = -\frac{1}{\sqrt{K_\infty}} \mathrm{e}^{\mathrm{i}(\omega/K_\infty)x} \widetilde{A}''(x). \tag{6.48}$$

It remains to substitute (6.48) into (6.46), and we can see that the pressure in the viscous sublayer is given by

$$\begin{aligned} \widetilde{P}(x) &= \mathrm{e}^{-\mathrm{i}(\omega/K_\infty)x} p_v|_{Y=0} \\ &= -\frac{1}{\sqrt{K_\infty}} \int_{-\infty}^{x} \mathrm{e}^{-\mathrm{i}(\omega/K_\infty)(x-\xi)} \widetilde{A}''(\xi) \mathrm{J}_0\left(\frac{\omega}{K_\infty}(x-\xi)\right) \mathrm{d}\xi. \end{aligned} \tag{6.49}$$

Equation (6.49) was used, together with (6.16) and (6.17), to analyse the receptivity process for $K_\infty > 0$.

Similar to the subsonic flow regime, the calculations were performed for the roughness shape $g(x) = hF(x)$ with $F(x) = \mathrm{e}^{-2x^2}$. The results of the calculations are shown in figure 12 in the form of the distribution of the pressure gradient along the body surface. We see that the Tollmien–Schlichting wave decays downstream if the acoustic wave interacting with the roughness has a subcritical frequency ($\omega = 2.6$) and grows for a supercritical frequency ($\omega = 3.25$). The results in figure 12(a) correspond to unit value of Kármán–Guderley parameter K_∞. Figure 12(b) shows that for $K_\infty = 1$ the neutral frequency is $\omega = 3.025$.

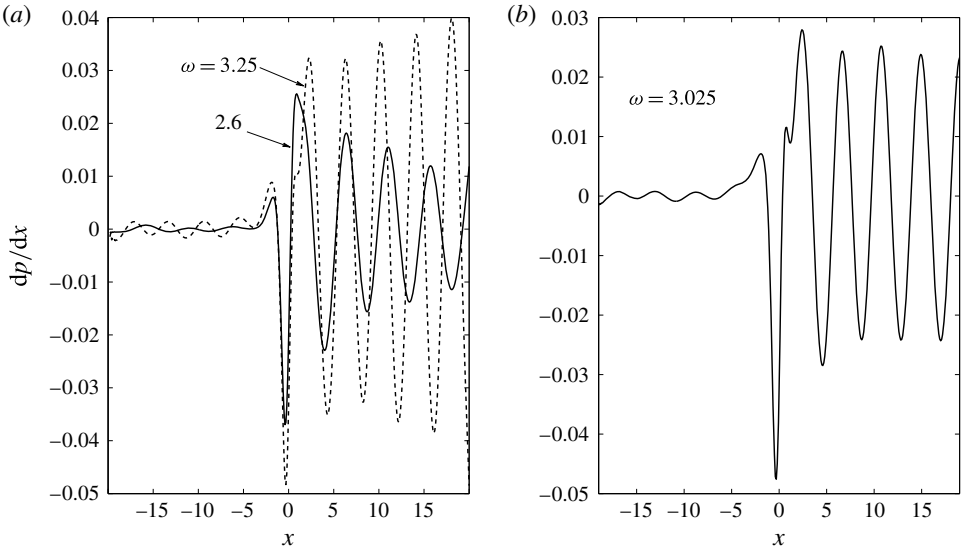

FIGURE 12. Pressure gradient distribution for three different acoustic wave frequencies ω, roughness hump height $h = 0.1$ and Kármán–Guderley parameter $K_\infty = 1$: (*a*) subcritical and supercritical frequencies; (*b*) neutral perturbations.

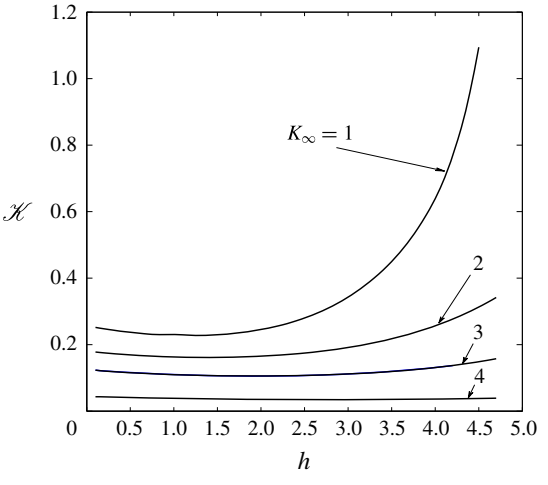

FIGURE 13. The receptivity coefficient $\mathscr{K}$ for $K_\infty > 0$.

The calculations were repeated for a number of values of the Kármán–Guderley parameter in the range $K_\infty \in (0, 5)$, and for various values of the roughness height h. The results of these calculations are summarised in figure 13, where the receptivity coefficient $\mathscr{K}$ for neutral Tollmien–Schlichting waves is displayed. Interestingly, the receptivity coefficient does not show the same growth with h as for the subsonic flow regime (see figure 11).

7. Discussion of the results

This work is concerned with the generation of the Tollmien–Schlichting waves in the boundary layer on a wing surface in the transonic flow regime. Assuming that

the Reynolds number is large, we use the transonic version of the viscous–inviscid interaction theory, which is known to describe the stability of the boundary layer on the lower branch of the neutral curve. It is assumed that the Tollmien–Schlichting wave is generated through interaction of the acoustic wave impinging upon the boundary layer with steady flow perturbations produced in the flow by a small wall roughness. The results of the analysis confirm, once again, that effective generation of the Tollmien–Schlichting waves takes place when the so-called double-resonance condition is observed. This condition requires that (i) the frequency of the acoustic wave is tuned to the frequency of the Tollmien–Schlichting wave, and (ii) in the Fourier spectrum of the steady perturbations produced by the wall roughness there is a harmonic with wavenumber that coincides with the wavenumber of the Tollmien–Schlichting wave. The transonic version of the triple-deck theory is applicable when the free-stream Mach number M_∞ is such that $M_\infty - 1 = O(Re^{-1/9})$. In this flow regime, the dimensionless frequency of the Tollmien–Schlichting wave is an $O(Re^{2/9})$ quantity and wavelength is estimated as $O(Re^{-1/3})$.

We first develop the linear receptivity theory. It is applicable when the amplitude of the pressure perturbation in the acoustic wave is small compared to $\rho_\infty U_\infty^2 Re^{-1/9}$, and the roughness height is small compared to $LRe^{-11/18}$. Under these conditions, the governing equations my be solved in an analytic form. As a result, an explicit formula for the amplitude of the generated Tollmien–Schlichting wave is deduced. It can be expressed as the product of the so-called receptivity coefficient and the Fourier transform of the roughness shape calculated for wavenumber of the Tollmien–Schlichting wave. The former does not depend on the roughness shape, and reaches a maximum when the Kármán–Guderley parameter K_∞ becomes zero or, equivalently, the free-stream Mach number $M_\infty = 1$.

In the second part of the paper, we lift the restriction on the roughness height, allowing the basic flow to develop a local separation region near the roughness. For this case the analysis of the generation of the Tollmien–Schlichting waves is conducted through numerical solution of the viscous–inviscid interaction problem. First, the basic steady flow is calculated for various values of the Kármán–Guderley parameter K_∞, progressively increasing the roughness height. Then the flow response to the impinging acoustic wave is determined through numerical solution of the unsteady viscous–inviscid interaction problem. The numerical method used in this study is based on Newtonian iterations where the solutions in the viscous and inviscid parts of the flow are calculated assuming that the displacement function is known. The iterations are conducted to adjust the displacement function such that it would make the pressure distributions in the viscous and inviscid flow coincide with one another. The results of the calculations show that for negative K_∞, when the flow outside the boundary layer is subsonic, the receptivity is enhanced significantly by the formation of a separation region. Surprisingly, in the supersonic flow regime ($K_\infty > 0$) the separation has only a moderate effect on the receptivity process.

In conclusion, we shall make the following comment. The asymptotic approach used in this paper is primarily intended to uncover the fundamental physical processes involved in the receptivity process. At the same time, we know from a number of comparisons of the triple-deck theory with the Navier–Stokes simulations of the boundary-layer receptivity in subsonic flows that the triple-deck predictions are rather accurate (see e.g. Tumin 2006; Tullio & Ruban 2015). Therefore, we expect the results presented in this paper to be sufficiently accurate for engineering applications.

Acknowledgements

This research was performed in the Laminar Flow Control Centre (LFC-UK) at Imperial College London. The centre is supported by EPSRC, Airbus UK and EADS Innovation Works.

REFERENCES

ABRAMOWITZ, M. & STEGUN, I. A. 1965 *Handbook of Mathematical Functions: With Formulas, Graphs and Mathematical Tables*. Dover.

BERNOTS, T. 2014 Receptivity of the boundary layer in transonic flow past an aircraft wing. PhD thesis, Imperial College London.

BOGDANOV, A. N., DIESPEROV, V. N., ZHUK, V. I. & CHERNYSHEV, A. V. 2010 Triple-deck theory in transonic flows and boundary layer stability. *Comput. Math. Phys.* **50** (1), 2095–2108.

BOWLES, R. I. & SMITH, F. T. 1993 On boundary-layer transition in transonic flow. *J. Engng Maths* **27**, 309–342.

GOLDSTEIN, M. E. 1983 The evolution of Tollmien–Schlichting waves near a leading edge. *J. Fluid Mech.* **127**, 59–81.

GOLDSTEIN, M. E. 1985 Scattering of acoustic waves into Tollmien–Schlichting waves by small streamwise variations in surface geometry. *J. Fluid Mech.* **154**, 509–529.

KRAVTSOVA, M. A., ZAMETAEV, V. B. & RUBAN, A. I. 2005 An effective numerical method for solving viscous–inviscid interaction problems. *Phil. Trans. R. Soc. Lond.* A **363** (1830), 1157–1167.

LIN, C. C. 1946 On the stability of two-dimensional parallel flows. Part 3. Stability in a viscous fluid. *Q. Appl. Maths* **3**, 277–301.

RUBAN, A. I. 1984 On the generation of Tollmien–Schlichting waves by sound. *Fluid Dyn.* **19**, 709–717.

RUBAN, A. I., BERNOTS, T. & PRYCE, D. 2013 Receptivity of the boundary layer to vibrations of the wing surface. *J. Fluid Mech.* **723**, 480–528.

RYZHOV, O. S. 2012 Triple-deck instability of supersonic boundary layers. *AIAA J.* **50**, 1733–1741.

SCHUBAUER, G. B. & SKRAMSTAD, H. K. 1948 Laminar-boundary-layer oscillations and transition on a flat plate. *NACA Tech. Rep.* TR 909.

SMITH, F. T. 1979*a* Nonlinear stability of boundary layers for disturbances of various sizes. *Proc. R. Soc. Lond.* A **368**, 573–589.

SMITH, F. T. 1979*b* On the nonparallel flow stability of the Blasius boundary layer. *Proc. R. Soc. Lond.* A **366**, 91–109.

TERENT'EV, E. D. 1981 The linear problem of a vibrator in a subsonic boundary layer. *Z. Angew. Math. Mech.* **45**, 791–795.

TIMOSHIN, S. N. 1990 Asymptotic form of the lower branch of the neutral curve in transonic boundary layer. *Uch. Zap. TsAGI* **21** (6), 50–57.

TULLIO, N. & RUBAN, A. I. 2015 A numerical evaluation of the asymptotic theory of receptivity for subsonic compressible boundary layers. *J. Fluid Mech.* **771**, 520–546.

TUMIN, A. 2006 Biorthogonal eigenfunction system in the triple-deck limit. *Stud. Appl. Maths* **117**, 165–190.